R. & M. No. 3457

MINISTRY OF AVIATION

AERONAUTICAL RESEARCH COUNCIL

REPORTS AND MEMORANDA

Wind Tunnel Tests of a Wing Fitted with a Single Lifting Fan

By N. GREGORY, M.A., W. G. RAYMER, B.SC. and EDNA M. LOVE

LONDON: HER MAJESTY'S STATIONERY OFFICE

1967

PRICE £1 4s. 6d. NET

Wind Tunnel Tests of a Wing Fitted with a Single Lifting Fan

By N. GREGORY, M.A., W. G. RAYMER, B.Sc. and EDNA M. LOVE

Reports and Memoranda No. 3457*
December, 1964

Summary.

Results are given of wind-tunnel tests of a square wing with a lifting fan of 1/44th the wing area located at 0·354 chord. Forces and pressure distributions were measured both on the bare wing and with plain and split flaps. A loss of flap effectiveness is noted for a very limited combination of plain flap deflection and advance ratio. An analysis is given of the flow through the fan and the total head rise is related to the local conditions at entry and exit.

Tests with a cascade in the fan duct at exit to deflect the efflux are described and the results are presented in a form that shows an economy in power requirements up to 20 deg jet deflection.

The forward-speed lift characteristics are greatly affected by fitting underfins of a suitable size and disposition, tangential to the duct exit. The loss of lift at low forward speeds can be completely eliminated by these means.

LIST OF CONTENTS

*Replaces A.R.C.26504

Introduction

The present report gives a description of the results of wind-tunnel tests of a square wing with a fan located at 0·354 chord [$\delta(2)$]. Some of the force data have already been issued without detailed comment by way of example to Ref. 1. The model was built primarily to allow an examination to be made of features of the internal flow and a paper has already been issued[2] on this aspect which includes the examination of the mal-distribution of the flow through the fan due to forward speed and the effect of an inlet cascade in diminishing it. The secondary aim of an examination of the external aerodynamics and of the effects of the interaction between mainstream and jet efflux is dealt with here. The model was made large in relation to the fan area in order to accentuate these possible interactions and is thus somewhat unrepresentative of a full-scale application of the lifting fan principle, though closer in proportions to what might be constructed if a lifting-fan unit were installed near a wing tip for control purposes. The model is also overlarge in relation to the tunnel size, so that in the absence of tunnel corrections, the results should be regarded as an approximation to those obtaining in ground effect.

The paper also discusses measures which were taken in order to modify the overall force characteristics. These include the deflection of the fan efflux by means of a flat plate cascade on the lower surface of the wing, and the use of fences to alter the interaction between jet efflux and mainstream.

The present series of tests had been preceded by preliminary tests on a wing (of rectangular planform) of aspect ratio 2 with a relatively even smaller fan located further aft at 0·425 chord, and also on a swept wing project with only the apex fan (out of an intended three fans) fitted. The results of these tests were given in a number of unpublished data reports[3,4,5]. The main results are here briefly re-capitulated in an Appendix, thus enabling comparisons to be made between the models and preliminary conclusions to be drawn about the effects of fan location and ratio of fan area to wing area.

2. *Model Details and Experimental Arrangements.*

The model consisted of a symmetrical 15 per cent thick square wing with both chord and basic span of 64 in., plus wing-tip fairings of semi-circular cross-section. The aerofoil section was derived from NACA 0020 by adding a constant thickness region which extended over the chordwise length of the fan aperture. The model was fitted with a 20 per cent plain flap and provided with split flaps which could be attached externally at 30 deg and 60 deg deflections. A general arrangement of the model, which was built by Messrs. Boulton Paul Aircraft Ltd., is shown in Fig. 1. Pressure-plotting holes were also fitted along the centre line of the model and along lines 0·82 fan diameters on either side of the centre line, and also on circles round the fan axis at 1·63 and 2 fan diameters.

The fan had a diameter, d, of 13·16 in. with a hub/diameter ratio of $\frac{1}{2}$ and was fitted in the wing with its axis normal to the chord line at 0·354 chord from the leading edge along the centre line of the model. The fan was designed and constructed by Messrs. Armstrong Siddeley Motors Ltd. and had 20 inlet guide vanes with zero camber and outlet angles, a rotor with 21 blades and a stator with 20 blades, both with circular arc aerofoils. The complete blading design is given in Table 1 which also gives the design performance specification.The fan was located near the top of its duct, as is shown in Fig. 2, 2·6 in. or 20 per cent duct diameter below the surface. The duct commenced with an inlet flare of lip radius 1·3 in. or 10 per cent of the duct diameter. Except when the inlet cascade shown in Fig. 2a was in use, the fan hub was faired with a bluff boss with lip radius of 1 in. and the hub terminated immediately downstream of the stator blade trailing-edge plane without any tail cone.

The fan was driven by a direct current electric motor buried in the wing, via a $\frac{3}{8}$ in. diameter extension shaft and bevel reduction gearing in the hub. The shaft crossed the annulus midway between two of the stator blades, and this was found seriously to disturb the flow through the fan.

The fan hub boss and bottom plate were provided with fittings to locate rakes of three five-tube yawmeters which could be mounted either immediately upstream or downstream of the fan unit. The rakes could be rotated about the fan axis into any of 20 equally spaced positions by means of a hollow shaft which extended outside the tunnel and carried the pressure leads. The shaft was supported on a bearing at the hub of a tripod which was screwed to the surface of the wing. Means were provided for altering the radius of the probes. which were normally carried at 15, 50 and 85 per cent of the annulus width, and for

adjusting the angular position of the probes in each sector, which was normally midway between each pair of stator blades. The probes were kept aligned parallel to the axis of the fan and were used in this position, having previously been calibrated over a range of ± 30 deg by rotation of the probe arm about the appropriate axes when protruding through the wall into the working section of a 1 ft wind tunnel. The plane of the probe heads on the upstream side was 1·45 in. below the upper surface of the wing and 1·15 in. above the inlet guide vanes, and on the lower surface, 0·15 in. below the stator blades and 3·5 in. above the lower surface of the wing. Check traverses were also carried out with the probe heads in the plane of the lower surface of the wing. The traverses enabled estimations to be made of the mass flow through the fan and of the work done on the efflux by the fan. Electrical power input and torque measurements were not made.

The tests were carried out with the model suspended from the roof balance, first in the N.P.L. Duplex wing tunnel (14 ft × 7 ft), and, following the demise of the tunnel in 1959, also in the 13 ft × 9 ft wind tunnel. The wing was the right way up with jet efflux directed towards the floor and the centre-line of the wing was 45·1 in. above the floor of the Duplex wing tunnel (0·54 × Tunnel height) and 60 in. above the floor of the 13 ft 9 ft tunnel (0·55 × tunnel height). Small differences therefore arose between the force measurements obtained in the two tunnels. These measurements are presented uncorrected for tunnel constraint, since appropriate corrections for models with lifting fans were not available. As pointed out by Wyatt[6], the corrections differ from those for a conventional model, and are more numerous. In any case, the chief correction will be that due to the presence of the tunnel floor. As this correction is omitted, the results may be regarded as being close to what would be obtained when flying in ground effect, which is the case immediately after take-off, and therefore of considerable interest.

3. *Presentation of Results.*

There are various possible ways of correlating the measurements, as is pointed out in Ref. 1, and the graphs which illustrate this report will make use of the convention best suited for the particular point at issue.

At times, one will be interested in the incremental forces ΔL, ΔD, due to the operation of the fan, measured above the values obtaining at the same forward speed with the fan apertures sealed. These forces can be rendered non-dimensional either by dividing by the incremental lift obtained at zero forward speed or by dividing by $\rho A_F V_F^2$ which is approximately* the momentum flux through the fan and varies with forward speed V, even when the fan rotational speed is kept constant. In this system the forward speed is measured as a proportion of the flow speed through the fan, V_F.

In dealing with questions of jet efflux deflection, where there is an exchange between lift and drag, or for performance analysis of a complete aircraft, it is necessary to consider overall forces. The system introduced in Ref. 1 is here used: the non-dimensional parameters are

the fan speed parameter, $\pi nd(\frac{1}{2}\rho A_F/L)^{\frac{1}{2}}$ $(= 1/\sqrt{C_T})$

the drag/lift ratio, D/L

and the chordwise position, x/c, of the centre of pressure $(= M/Lc)$

which are functions of

the incidence, α

flap deflection η

and the forward speed parameter, $V_T\,(\frac{1}{2}\rho A_W\,L)^{\frac{1}{2}}$ $(=1/\sqrt{C_L})$

*The approximation is explained in Section 6.

The fan torque was not measured in the present experiment so that accurate measurements of power input to the fan were not available. However, the work done on the fan efflux could be estimated from the traverse measurements so that the fan output power, P, could be expressed in terms of a coefficient

$$K_p[= P/\tfrac{1}{2}\rho A_F(\pi nd)^3]$$

which was found to be a function of μ $(= V_T/\pi nd)$, the ratio of forward speed to fan blade tip speed. For very low values of μ, K_p will be found to be independent of incidence, and the gradient $dK_p/d\mu$ to be zero, as might be expected.

Treating the present wing model as if it were a complete aircraft, and assuming that it is fitted with an ideal thrust producing mechanism with known actuator disk area (here taken as equal to the fan disk area), it is possible to evaluate an ideal power output ratio as a measure of the power required to maintain flight at various stages of transition. This value, ξ, is defined as the ratio of the sum of the fan's rate of doing work on the efflux relative to the aircraft plus the thrust engine's rate of doing work on the slipstream to the hovering value of the former when supporting the same weight of aircraft at zero incidence. The algebraic expression for ξ is

$$\xi = \frac{P + \left[\tfrac{1}{2}T_e V_T + \sqrt{\left(\tfrac{1}{4}T_e^2 V_T^2 + \tfrac{1}{2}\frac{T_e^3}{A_T\rho}\right)}\right]}{P_0\left[\dfrac{L\cos\alpha + D\sin\alpha}{(L_0\cos\alpha + D_0\sin\alpha)\left[\cos(\Gamma+\alpha) - N\sin\alpha\right)}\right]^{\frac{3}{2}}} \tag{1}$$

where the required thrust,

$$T_e = \frac{D\cos\Gamma + NL + L\sin\Gamma}{\cos(\Gamma + \alpha) - N\sin\alpha} \tag{2}$$

and the weight of aircraft supported

$$W = \frac{L\cos\alpha + D\sin\alpha}{\cos(\Gamma + \alpha) - N\sin\alpha} \tag{3}$$

and the suffix $_0$ refers to hovering conditions at incidence α. In these expressions Ng is the acceleration of the aircraft, Γ is the angle at the flight path to the horizontal and A_T is the area of the thrust engine actuator.

4. *Force and Pressure Measurements on the Plain Wing,*

Lift, drag and pitching moments were measured in the Duplex wind tunnel at 4 deg intervals over the incidence range -12 deg to $+12$ deg and at forward speeds up to 50 ft/sec on the plain wing with fan aperture sealed, with it open and with the fan running at 41·7 revs/sec. The results are listed in Table 2. At zero incidence, a range of fan rotational speeds between 21·7 and 41·7 revs/sec was covered and closer intervals were taken in tunnel speed than at the other incidences. Wind speeds below 25 ft/sec were obtained for the first time in the series of tests on fan wings by the artifice of introducing distributed blockage into the tunnel 28 ft downstream of the model.

Fan-off results with the fan duct sealed at both ends are illustrated in conventional coefficient form in Fig. 3, and as a matter of interest, the increments in the coefficients due to opening the fan aperture are given in Fig. 4.

The variation with wind speed of the lift and drag increments (relative to duct sealed conditions) due to fan operation with the wing at zero incidence are shown in Fig. 5 for the various fan rotational speeds and the results have been rendered non-dimensional in terms of the momentum flux through the fan in Figs. 6 and 7. Fig. 8 shows the corresponding variation of the ratio of drag increment to lift increment. The non-dimensional moment increment is plotted in Fig. 9 and the result is illustrated another way in Fig. 10 which gives the chordwise position at which the lift increment due to the fan acts.

The effect on the incidence on the lift, drag and pitching moment increments due to fan operation is shown in Figs. 11–15. In order to avoid confusion, staggered zeros have been used for the curves in Figs. 11 and 14.

The reduction of the overall forces by the method recommended in Ref. 1 is shown in succeeding graphs. Figs. 16, 17, 18 and 20 show the variation with forward speed parameter of the fan speed parameter, lift-drag ratio, centre of pressure and ideal output power ratio, whilst Fig. 19 shows the ideal fan output power coefficient K_p as a function of μ, the ratio of forward speed to fan blade tip speed which principally determines the operating point of the fan on its characteristic.

Force measurements on the plain wing were accompanied by a somewhat incomplete set of surface pressure measurements. On the chordwise line through the fan axis the pressure coefficient distribution was obtained at forward speed ratios V_T/V_F of 0·34, 0·62, 0·925 and fan off, as is shown in Fig. 37a to d, which also includes the effect of flap deflection. On the lower surface alone, pressure distributions were obtained along the centre line as far as the flap hinge position and also along lines $\pm 0{\cdot}168$ chord ($\pm 0{\cdot}815$ fan diameter) on either side of the centre line at V_T/V_F values of 0·24, 0·44 and 0·68 as shown in Fig. 21. Additional pressure points in the lower surface were included which enabled circumferential distributions of the pressure to be plotted in Fig. 22 at radii 1·63 and 2 times the fan radius. Lower surface pressure distributions along lines radiating from the fan axis are plotted for a value of V_T/V_F of 0·55 in Fig. 23. This speed ratio is one for which complete fan traverses were available, including an additional set in the plane of the lower surface. The measurements of static pressure given in Fig. 23 outside the duct were interpolated, both with respect to position and velocity ratio, from the data of Figs. 21 and 22. The eight radial positions used in Fig. 23 were uniformly spaced except that the spanwise directions have been replaced by directions with angular displacement of 111 deg and 255 deg from the upstream direction, which were the two actual fan traverse positions out of the twenty taken in which the static pressures were least.

5. *Performance of the Lifting Unit,*

This section attempts to extend the analysis given in Ref. 2 of the performance of the lifting fan unit by relating it to the aerodynamics of the wing, by correlating the yawmeter traverses taken in the fan duct upstream and downstream of the fan with the pressure plotting measurements on the wing, and with the overall force measurements obtained on the balance. The traverse measurements were primarily undertaken to examine the mal-distributions that occurred at forward speed, reported in Ref. 2, and whilst adequate for this purpose, prove to be insufficiently extensive and reliable for a fully detailed, self-consistent picture of the interacting flows to be built up.

Difficulties arising from the instrumentation are discussed in Ref. 2. It is thought that the estimation of static pressure and total head from the yawmeter readings was not very reliable on the inlet side as large flow angles in pitch and yaw were present simultaneously and a full calibration of the yawmeters had not been carried out in these conditions. The accuracy in measurement of total head was estimated to be only to 2 per cent of $\frac{1}{2}\rho V_F^2$ and in static pressure to be somewhat worse. Further difficulties in discussing changes that occur across the fan disc arise from the axial thickness of the stator-rotor-stator combination which permitted non-axial flow to occur between upstream and downstream fan traverse planes.

The mean axial flow speed through the fan, V_F, has been worked out from traverses both immediately upstream and downstream of the fan unit and there is about 6 per cent difference in the results in the range over which the inlet traverses could be evaluated. Above a value of V_T/V_F of about 0·55 evaluation was impossible as the flow angles at inlet exceeded the limit of calibration of the yawmeter. The velocity given

by the inlet traverse is taken to be the correct value of the mean flow speed. The exit traverse gives a high value because no allowance was made for the boundary layers on the stator blades, hub and duct walls, which were entirely outside the 60 yawmeter positions used, or for the velocity variation over each sector (measurements having been made only at three points in the region of maximum speed in the middle of each sector). In the sector crossed by the drive shaft the yawmeter readings were falsified by the total head gradient due to the wake of the drive shaft, though in tests at forward speeds the wake had evidently shifted slightly, clear of the yawmeter tube in the outer radial position.

The variation of the non-dimensional parameter $V_F/\pi nd$ with $V_T/\pi nd$ is shown in Fig. 24 for both upstream and downstream traverses. The exit value of the mean flow speed (used in the Appendix) is referred to as the *nominal* speed, $V_{F_{nom}}$, and the true speed has been taken as 94 per cent of this at all advance ratios. Fig. 24 also shows the variation with advance ratio of the standard deviation , σ, of the velocity measurements, both at inlet and exit. This quantity is necessary because throughout all the report except Table 3, weighted mean velocity V_F has been used in formulating $\rho A_F V_F^2$ for rendering lift, drag and pitching moment increments non-dimensional, as well as for determining V_T/V_F. The momentum flux is strictly $\rho A_F \overline{V_F^2}$ where $\overline{V_F^2}$ is the mean of the velocity squared, and the ratio of momentum flux to $\rho A_F V_F^2$ is $1 + \sigma^2$. From Fig. 24 it may be shown that up to V_T/V_F of 0·55, the momentum flux is actually 2 to 3 per cent in excess of $\rho A_F V_F^2$, but that as V_T/V_F rises to values of 0·8 and 1·2 the momentum flux excess over $\rho A_F V_F^2$ rises to 14 per cent and 36 per cent.

Analyses of the lift experienced by a lifting-fan/wing model based on momentum considerations can be made in two ways.

In the first approach, we consider the change of momentum of the fluid crossing the two planes 0 and 2, Fig. 25a, where 0 is far removed from the wing and 2 envelops the lower surface of the wing cutting the fan duct in the stator trailing edge plane.

Under static conditions we obtain

$$Thrust = \int (\rho V_F^2 + p_2 - p_0) dA \tag{4}$$

where the integral is restricted to the whole duct area (including hub) if the assumption is made that the static pressure over the rest of the lower surface is equal to the undisturbed static pressure p_o and that no fluid crosses the plane 2 other than in the duct. In the terminology of the Definitions Panel[7], the thrust is the net standard thrust.

Now Bernouilli's equation upstream of the fan gives

$$p_0 = p_1 + \tfrac{1}{2}\rho V_F^2 \tag{5}$$

and the total head rise across the fan is

$$\Delta H = p_2 - p_1 = p_2 - p_0 + \tfrac{1}{2}\rho V_F^2. \tag{6}$$

The force on the rotor and stator blades

$$\begin{aligned} &= \Delta H\, A_F \\ &= A_F(p_2 - p_0 + \tfrac{1}{2}\rho V_F^2) \\ &= A_F(\rho V_F^2 + p_2 - p_0) - \tfrac{1}{2}A_F\rho V_F^2 \\ &= Thrust \quad - A_H(p_2 - p_0) - \tfrac{1}{2}A_F\rho V_F^2 \end{aligned}$$

since the thrust is given by equation (4) and includes contributions across the annulus A_F and also the hub, A_H, where V_F is locally zero. This equation may be re-written as

$$Thrust = Blade\ load + A_H(p_2 - p_0) + \tfrac{1}{2}A_F\rho V_F^2 \tag{7}$$

and the second term on the right hand side is clearly a hub-suction due to the bluff downstream termination of the hub, and the last term is the lift developed on the upper surface of wing and hub, i.e., shroud force.

Hence,

$$\frac{\textit{Shroud force}}{\textit{Thrust}} = \frac{\frac{1}{2}A_F\rho V_F^2}{A_F(\rho V_F^2 + p_2 - p_0) + A_H(p_2 - p_0)}$$

$$= \frac{1}{2 + \left(\frac{A_F + A_H}{A_F}\right)\frac{p_2 - p_0}{\frac{1}{2}\rho V_F^2}} \tag{8}$$

The ideal case of a large wing surrounding the fan duct, ensures that the inflow velocities at the wing leading and trailing edges are small and that there is therefore no violation of the assumption that no momentum flux occurs across the section (2) except in the fan duct. One can then see from equation (8) that if the hub area is negligible so that there is no diffusion of the flow in the fan duct and $p_2 = p_L = p_0$ there is a maximum value of the shroud force equal to half the total force.

For the present wing, the exit area $A_F + A_H = \frac{4}{3}A_F$, so that if the duct flow diffused without loss, $(p_L - \bar{p_2})/\frac{1}{2}\rho V_F^2$ would equal $(1 - \frac{9}{16}) = 0{\cdot}4375$. Ideally, with $p_L = p_o$, the ratio shroud force/total force could rise to $\dfrac{1}{2 - \frac{4}{3} \times \frac{7}{16}} = 0{\cdot}706$.

As the hub was bluff, no such pressure recovery took place. Traverses in the plane of the lower surface were made under static conditions and at a forward speed ratio V_T/V_F of 0·55. In both cases a pressure rise coefficient of 0·117 was measured in the duct below the fan, only 27 per cent of the possible rise. Furthermore, the lower surface traverse showed that the static pressure fell towards the axis of the duct due to the flow expanding to fill the cavity downstream of the hub. Although at the outer edge of the duct, p_L was substantially equal to p_0, the mean value of $\dfrac{p_L - p_0}{\frac{1}{2}\rho V_F^2}$ was equal to $-0{\cdot}083$.

$$\text{Hence } \frac{p_0 - p_2}{\frac{1}{2}\rho V_F^2} = 0{\cdot}117 + 0{\cdot}083 = 0{\cdot}200 \text{ and the ratio}$$

$$\frac{\textit{Shroud force}}{\textit{Total force}} = \frac{1}{2 - \frac{4}{3} \times 0{\cdot}20} = 0{\cdot}578.$$

The balance and traverse measurements taken at zero forward speed are included in Table 3. Under static conditions the measured lift is 0·59 lb less than the net standard traverse thrust, but this discrepancy was changed in sign when the tunnel floor boards were removed and re-circulation of the efflux ceased, for the lift measured on the overhead balance rose by 1·15 lb to 10·8 lb. The fact that there was still a discrepancy suggests that the assumption that there is no momentum flux across plane 2 except in the duct is incorrect. This explanation is further strengthened by the fact that the highest possible estimate of the shroud force, *viz.* 10·8 – 5·68 lb is still only 47 per cent of 10·8 lb.

Little progress can be made with this analysis at forward speeds. It can be argued by superposition of a flow over the upper surface on top of the inflow to the fan in the static case, that if the velocity over the upper surface is constant, or has fore and aft symmetry with regard to the fan axis, then the shroud force developed would remain equal to $\frac{1}{2}\rho A_F V_F^2$. However, Table 3 shows that the difference between the blade load and the lift – either that measured on the balance or the estimated net standard traverse thrust – is not constant. In the next section it is further shown that the above superposition is incon-

sistent with the measured pressure distributions. At forward speeds it becomes impossible to separate the pressure forces acting on the wing into components due to lower surface interactions, upper surface shroud effect, and forces due to any changes of circulation or changes in tunnel constraint.

The alternative (but equivalent) approach is to apply the momentum equation to a circuit which closely envelops the wing and cuts across the fan duct in the upstream and downstream traverse planes, Fig. 25b, whence

Total lift (*fan on*)	=	*Pressure lift on aerofoil and hub*	+	*Pressure lift across fan annulus* ($\int \Delta H \, dA$)
(1)		(2)		(3)

The balance and traverse measurements taken at various forward speeds at a fan rotational speed of 41·7 revs/sec (except where noted) have been evaluated and are presented in this way in Table 3. Again, no check on consistency is possible since although (1) represents the balance measurement, and (3) is calculated from the total head traverse measurements, (2) can only be obtained as a difference because no static pressure measurements were made on the hub and those on the surrounding wing only covered a small spanwise extent. A further minor approximation implicit in the equation is that the momentum fluxes into and out of the fan are assumed equal. The mass flow clearly is the same, but at high forward speeds, it is possible that the smoothing effect of the fan would reduce the standard deviation of the velocity measurements between inlet and exit sufficiently to alter the momentum flux. As already explained, this could not be checked as the yawmeter traverse on the inlet side could not be evaluated above a value of V_T/V_F of 0·55 owing to the excessive flow angles.

An interesting feature of the force measurements given in Table 3 is the constancy of the net standard thrust over a considerable range of forward speeds. However, an extension of the argument using equations (4) and (6) shows that this is fortuitous and due to the particular value of the gradient of the fan characteristic, (given in Fig. 2 of reference 2). The mean total head and static pressures at the two traverse planes are also given in Table 3 and are plotted in Fig. 26: They are expressed in terms of the dynamic pressure of the mean fan flow velocity. The head loss coefficient of the inflow is negligible at small forward speeds and rises to 6 per cent at V_T/V_F of 0·55, beyond which it was impossible to evaluate the yawmeter traverses owing to the large flow angles. Note that this loss coefficient ignores the losses in the boundary layers on the duct walls. The total head rise demanded of the fan appeared to decrease with increasing forward speed though the point at which it became zero could not be determined precisely on account of the unknown behaviour of the inlet loss coefficient above V_T/V_F of 0·55. (Note that for the calculations of Ref. 1, inlet losses had been ignored).

The mean static pressure on the lower surface over the area of the fan duct, both fan off and fan on, is shown in Fig. 26. The area 'A' indicates a lower surface suction which tends to increase the mass flow through the fan. Above V_T/V_F of 0·88 this tendency is reversed, a feature that, without modification of the exit, would inhibit auto-rotation of the fan for starting in flight. On the upper surface, the reduction in static pressure at the plane of the traverse due to the flow through the fan is indicated by the dimension 'B' This is greater than indicated theoretically, the excess 'C' being attributed to the considerable cross flow present at the traverse plane at high forward speeds, for the static pressure must be determined by the actual flow speed, whereas it is only the axial component of the velocity which determines the mass flow.

Circumferential distributions of static pressure above and below the fan and in the plane of the lower surface are shown for a value of $V_T/V_{F\,\mathrm{nom}}$ of 0·55 in Fig. 27. It is interesting to note that the peak suctions at azimuthal angles of 110 deg and 255 deg due to the jet/main-flow interaction which are prominent in the plane of the lower surface have little upstream influence as they are not present in the stator trailing edge plane. The peak pressure at the azimuthal angle of 0 (upwind duct generator), however, is felt at the stator plane, and indeed at the slightly higher forward speed ratio V_T/V_F of 0·88 provokes duct boundary-layer separation which affects the outer probe at $2r/d$ of 0·925 from azimuthal angles between 350 deg and 130 deg.

It can be seen in Fig. 23 that the peak suctions decrease rapidly with increasing radius, but it should not be overlooked that the downward force on the lower surface is given by $-\int C_p r dr$ and a considerable contribution to this comes from small static pressure changes at large radial distances.

6. *Discussion of Performance of Plain Wing.*

The behaviour of the wing with the fan duct sealed is normal. The lift curve slope at zero lift (neglecting any corrections for tunnel constraint) is 0·030 per degree (Fig. 3), a low value in excellent agreement with the figure of 0·029 which modern theories suggest[8] is appropriate for the aspect ratio of 1·15 (an effective value which includes the end fairings).

The simplest assumptions that can be made for discussing the wing behaviour with fan operating are that the fan flow can be superposed on the wing flow and that the fan flow on the exit side continues downward without interaction with the main stream. On this basis there would be a drag increment due to fan operation equal to the 'sink' drag of the flow into the fan. This is shown as a dotted line in Fig. 7 and is seen to be a possible approximation at low forward speed. At high forward speeds, however, the actual drag increment is considerably larger than the sink drag. Similar results from other wings are given in the Appendix. The lift increment $\Delta L/\rho A_F V_F^2$ would be independent of V_T/V_F and equal to 1 if there were no diffusion of the efflux downstream of the fan stator. The argument of the last section shows that $\Delta L/\rho A_F V_F^2$ [which is the same as (Total Force/2 × Shroud Force) of the last section] would be equal to 0·708 if the flow diffused without loss, or equal to 0·865 taking the mean measured pressure recovery between stator and lower surface. The latter value is marked in Fig. 6. The difference between this value and the experimental points can be ascribed partly to a variation in tunnel interference with forward speed and principally to the jet/mainstream interaction and circulation effects.

Another reason for abandoning an analysis based on momentum arguments is as follows. If there were no circulation changes it should be possible to superpose a flow over the aerofoil (fan off) with an inflow into the fan as was originally suggested in Ref. 9. An upper surface inflow coefficient can then be defined by

$$\frac{v_i}{V_T} = \sqrt{(1 - C_{p_{\text{fan on}}})} - \sqrt{(1 - C_{p_{\text{fan off}}})}$$

This has been evaluated for the present wing and is indeed independent of flap deflection as would be expected. But v_i/V_F [which is $(v_i/V_T)/(V_F/V_T)$] turns out ahead of the fan not to agree with any theoretical sink effect, nor aft of the fan even to be independent of V_F/V_T. Furthermore, v_i changes sign between x/c equal to 0·6 and 0·7 and aft of this point no longer represents an inflow. On the lower surface, a similar inflow coefficient v_i/V_T is not independent of flap setting. One concludes that interaction and circulation changes cannot be ignored.

Non-dimensionalising the force increments in terms of $\rho A_F V_F^2$ enables some comments to be made on Figs. 6–15, however. At forward speed ratios at which $\Delta L/\rho A_F V_F^2$ exceeds its static value, there is a slight spread in the plotted points. This can be seen in Figs. 6 and 15 and more markedly in Figs. 8 and 9. The spread consists of a small regular variation in the curve, associated with change of fan speed. This suggests some slight scale effect in fan performance in these cross flow conditions, or in the extent of boundary-layer separation over the intake lip or in the efflux/mainstream interaction.

Incidence effects at low forward speeds are merely the result of rotation of axes. Statically, the lift increment varies as cos α in Fig. 11 and the drag as sin α in Fig. 12. At high forward speeds, the drag increment is little affected by incidence (Fig. 12), but the lift increment (Fig. 11) is least at high incidence and greatest at large negative incidence as might be expected from the fact that the trailing jet path is closer to the lower surface of the wing at high incidences, which would lead to greater adverse interaction effects. It is also possible that some of the lift spread at high forward speeds is due to the variation with incidence of the pressure differential between upper and lower surface which the fan has to overcome,

which would affect the momentum flux and lift increment. This effect should not appear if ΔL had been non-dimensionalised by dividing by the actual momentum flux, but in the absence of traverses at high incidences, the zero incidence values were used. Fig. 24 shows that at V_T/V_F equal to 0·4, the measured variation in flow due to incidence scarcely exceeded the scatter of the measurements, but a larger effect would be expected at higher incidences.

The comment should also be made at this stage that the apparent fan lift bonus represented by the high values of $\Delta L/\rho A_F V_F^2$ obtained at high forward speed ratios V_T/V_F (Fig. 6) is relatively unimportant because under these conditions the fan is producing a lift increment which could be readily obtained by a small change in wing incidence. Fig. 16 shows that if a fixed weight of aircraft is being supported, the fan speed parameter for $\mu \geqslant 0{\cdot}4$ is well below its static value if the wing incidence is $\geqslant 4$ deg, and that the lifting system is entirely wing supported at slightly higher speeds. It is only for $\mu \geqslant 0{\cdot}4$, which corresponds to $V_T/V_F \geqslant 0{\cdot}6$ (Fig. 24), that the system yields high values of $\Delta L/\rho A_F V_F^2$ (Fig. 6).

The static pressure distributions measured on the lower surface of the model were not extensive enough in themselves to allow generalizations to be made. The measurements of pressure changes due to fan operation, however, have been found to be in good agreement with subsequent more detailed measurements of other investigators [10,11] using jets issuing from flat plates which reveal suction areas which would extend as far as the wing tips and trailing edge of the present wing. The R.A.E. measurements suggest that the pressure field to the rear of the fan does not vary very much between the centre line and the line distant $\pm 0{\cdot}168$ chord. An R.A.E. centre-line pressure distribution has been added to the fan-off distribution on the present wing at $V_T/V_F = 0{\cdot}24$ and is compared with the present measurement in Fig. 21a.

It should be noted that research work by Bradbury considers vorticity shed along an experimentally measured jet efflux path and gives calculated pressure distributions in good agreement with those just discussed.

The remaining effect of circulation changes about the wing has not yet been taken into account. Norland[12] has considered a potential flow theory for two-dimensional flow through an aerofoil which qualitatively indicates the measured characteristics, but this would not be at all appropriate to the case of a fan duct whose diameter is small with respect to both span and chord. It may be that for this particular case, circulation effects are far less important than the effects of the lower surface pressures induced by the efflux/mainstream interaction.

7. *Measurements on Wing with Deflected Plain and Split Flaps.*

The force measurements obtained in the Duplex wing tunnel with ± 15 deg of plain flap deflection and with 30 deg and 60 deg of split flap deflection are listed in Tables 4 and 5. Additional measurements, particularly with intermediate and with larger angles of deflection of the plain flap were taken in the 13 ft. × 9 ft. wing tunnel. These measurements are not tabulated here but are included as additional points on the graphs.

When the fan duct was sealed, flap deflection produces increments in lift, drag and pitching moment coefficient as shown in Fig. 28. These are all much as expected for a 20 per cent chord control on a wing of low aspect ratio.

The effect of plain flap deflection on the lift increment obtainable by running the fan is shown (with staggered scales) as a function of forward speed ratio in Fig. 29 and the corresponding drag and moment increments are given in Figs. 30 and 31. Above about 15 deg flap deflection the lift increment given by running the fan is much less at high forward speed ratios and becomes negative with 30 deg flap deflection and forward speed ratios greater than 0·6. With the same flap deflection and slightly lower forward speed a noticeable scale effect on lift increment is present. In the conditions where the lift increment is low or negative, the drag increment Fig. 30 is also reduced, but moment increments were not taken in these conditions.

The lift increments due to fan operation when either a 30 deg or 60 deg split flap was fitted are compared with the corresponding curve for a 30 deg plain flap in Fig. 32. The increments are less and become negative at a lower forward speed than is the case with the plain flap. The effect of change of incidence can also be seen. Corresponding curves for drag and moment increments are shown in Figs. 33 and 34.

The order of the curves of the lift increment due to fan operation with increase of forward speed does not of itself necessarily indicate a control reversal. It must be recalled that large flap and split flap deflections are very effective with the fan off as is shown by Fig. 28, and control reversal is concerned with the variation of total lift with flap deflection. What happens when a control is deflected at a constant forward and fan rotational speed is therefore best appreciated by reference to the relation between the dimensionless fan-speed and forward-speed parameters plotted in Fig. 35. Curves at constant incidence originally given in Fig. 16 are shown dotted, and curves for deflected plain and split flaps all refer to zero incidence. If a sudden change of wing incidence or flap deflection is made, the forward speed and fan rotational speed are not thereby altered. (The independence between fan speed and incidence or flap deflection at constant power is suggested by Fig. 19.) The operating point in Fig. 35 therefore moves from one characteristic to another along a radial line through the origin. If the direction of this movement is toward the origin for an increase in incidence or flap deflection, then the C_L is increased, implying an increase in lift at constant speed and positive values of $dC_L/d\alpha$ or $dC_L/d\eta$. It will be seen that negative values of the latter derivative indicating control reversal are only to be found between 20 deg and 30 deg plain flap deflection (where the curves cross) over the narrow forward speed range between μ values of about 0·25 and 0·5. The split flap data were taken at such widely spaced deflections that no reversal can be seen. Moreover, the similar shapes of the curves for 30 deg and 60 deg split flap deflections makes it unlikely that any reversal is present although the lift increments due to fan operation (Fig. 32) are very poor in these conditions. The variation of drag/lift ratio with forward speed and plain and split flap deflection is shown in Fig. 36. To avoid confusion, the effects of incidence variation have not been superimposed; these are given in Fig. 17.

Pressure plotting measurements were taken only along the centre line through the fan axis for the plain flap case, and distributions at three forward speed ratios and for the fan-off case are shown in Figs. 37a to d. Accompanying tuft observations on the centre line of the wing showed that on the upper surface of the flap the flow direction was towards the trailing edge for 0 deg and 10 deg flap settings, but at 15 deg flap deflection there was incipient separation from the upper surface of the flap. At 20 deg deflection the separation point moved progressively forward with increase of speed, from 0·97c at V_T/V_F equal to 0·34 to 0·83c at V_T/V_F equal to 0·93. At 30 deg deflection, the separation was at mid-flap (0·9c) for V_T/V_F equal to 0·34 and had reached the knee of the flap at V_T/V_F equal to 0·62.

On the lower surface, the tuft patterns at 30 deg flap deflection were less easy to interpret. At V_T/V_F values up to 0·24 the flow was attached and in the rearward direction except for a small separation bubble in the angle of the flap and very close to the fan duct itself where an entrainment inflow towards the duct predominated. At V_T/V_F equal to 0·34 the pressure rise along the lower surface was much greater and the flow separated completely, the tufts all pointing from the trailing edge towards the fan. With further increases in forward speed, the fan efflux passed closer to the flap so that the efflux, or some of the more slowly moving entrained air, impinged on the flap and formed an attachment region at about mid-flap chord separating the forward flow to the fan from a rearward flow to the trailing edge. It will be noted that the narrow speed range over which the flow is completely separated from the flap corresponds to the region of control reversal already commented on. It must be concluded that it is desirable to avoid fitting trailing-edge controls immediately downstream of a lifting fan.

8. *Effects of an Exit Cascade,*

Tests were carried out at zero incidence with a cascade of 12 flat plate vanes each of 1·1 in. chord fitted on the end of the fan duct with their hinges in the plane of the lower surface. At a given value of V_T/V_F, both lift and drag increments due to the fan with the cascade deflecting the efflux are different from those measured without the cascade. It is therefore necessary to use the non-dimensional system of force reduction based on overall forces. Fig. 38 shows the variation with forward speed of the fan speed parameter required to support a given weight for various exit cascade blade settings, β deg. Under static conditions the intercepts of Fig. 39 are closely equal to cot β for up to 30 deg blade deflection (i.e. $\beta \geqslant$ 60 deg), thus showing that the cascade is suitably deflecting the fan efflux. At larger angles of deflection

cot β is exceeded, through this may be due to an interaction between the emergent jet and the lower surface resulting in loss of lift. The effect of the cascade on the mass flow through the fan at constant fan rotational speed was only investigated with 30 deg deflection of the jet at 30 ft/sec forward speed. Under these conditions, the presence of the cascade reduced the flow by 8 per cent: the uniformity of the flow at the stator trailing-edge plane was little affected.

The thrust-producing effects of the cascades are demonstrated by the variation with forward speed of the drag/lift ratio shown in Fig. 39. The balance between loss of lift and gain of thrust can be seen from the effects of cascade deflection on the ideal output power ratio calculated on the same assumptions as previously and shown in Fig. 40 for those experimental observations where the drag remained positive. The denominator of the output power ratio refers to the power required for hovering at zero incidence without the cascade fitted, so that the departure of the 90 deg cascade blade setting case from unity in the hovering case reflects the small reduction in the flow through the fan in these conditions. At values of the forward-speed parameter less than 2·5, the greatest saving in total power is obtained with only 10 deg deflection of the efflux, and this saving is completely eliminated at deflections not much greater than 20 deg.

The way in which the above result is modified by changes in the assumptions underlying the calculations, i.e., by the disk area of the thrust actuator, and by the imposition of a horizontal acceleration, are discussed in Reference 1. The result was also changed by two modifications to the cascade during further tests, this time in the 13 ft × 9 ft tunnel. The result of deflecting only the rear half of the cascade is shown in Figs. 41 and 42. This was tried because only small ranges of angles of deflection of the whole cascade proved beneficial. Blade deflection reduces the effective duct area measured perpendicularly to the efflux and therefore puts up the back pressure. By deflecting only half the cascade it was hoped that the flow through the fan would not decrease so much, and that the flow in the front half of the duct would follow the rear flow of the same reasons underlying the Coanda effect. Figs. 40 and 41 show that in fact the thrust component is greatly reduced, but for a given blade setting, the power requirements are slightly lower for the deflected half cascade than for the completely deflected cascade.

The second modification was to separate the cascade from the lower surface of the aerofoil by one or two inches. It was hoped that this also would reduce the back pressure. In this case, 20 deg efflux deflection was clearly the optimum deflection, Figs. 43 and 44, with the smaller gap better at low forward speeds and the larger gap better at the higher forward speeds.

9. *Effects of Underfins.*

An initial attempt to alter the low-speed lift characteristics of the fan wing was made by fitting two flat-plate vertical fins or fences on the lower side of the wing surrounding the fan duct. The fins were tangential to the fan duct with their leading edges about $\frac{1}{3}$ of the fan diameter back from the front of the duct. The fins were of constant depth for a chord of two fan diameters and then tapered back to the trailing edge of the wing. Three depths of fin were tried, one half, one, and two fan diameters. The loss of lift up to V_T/V_F of 0·3 exemplified by Fig. 6 was progressively reduced with increasing depth of fin. It was thought that a two-diameter depth of fin was larger than could conveniently be fitted so further tests were conducted varying the plan form and position of fins one and a half diameters deep.

The variation with forward speed of the lift and drag increments due to operating the fan in the presence of the fins are shown in Figs. 45 and 46 in terms of the lift increment due to the fan under static conditions without the fins, at the same fan rotational speed. In Fig. 47 is shown the ratio of the drag increment to the lift increment. These results show that the minimum fin surrounding the duct exit, (A, Fig. 45) gives a flat lift characteristic, whilst a forward extension of the fin (B) yields a rising characteristic, but a backward extension alone (C) has an adverse effect. The best lift characteristic is produced by the full-chord fins (D). These, however, produce the least reduction in drag compared with no fins, the biggest reductions coming from minimum fins (A). In consequence, there is little to choose between 3 of the fin patterns (A, B, D) as far as the ratio of incremental drag to incremental lift is concerned, Fig. 47.

From the point of view of practical application, it could be argued that the fins would be retractible and that the increments due to running the fan in the presence of the fins should be measured above the lift and drag obtained on the bare wing with the duct sealed, thus taking into account the drag of the fins themselves. In fact, adding the fins to the wing produces small increments of drag and lift, but even when these are taken into account as suggested, the relative positions of the curves in Figs. 45 to 47 are quite unaffected.

The mechanism by which these fins work has been established by observation of tufts fitted on the present fins and held on a wand, and also by means of oil-flow and smoke visualisation techniques in other experiments [14,15,16]. The jet efflux spans the space between the two fins. The mainstream approaching the centre line of the jet between the fins is thus forced to turn vertically downwards instead of flowing round the efflux (Fig. 48). The pressure on the wing between the fins ahead of the duct is therefore greatly increased (*see* Figs. 49 and 50 compared with Fig. 21). The effect of this flow is that the fins act as loaded swept-back wings and shed vortices from their leading or tip edges, depending on the wind speed, Fig. 48a. The interaction between the fan efflux and the mainstream leads to the rolling up of a vortex other experiments[13,14,15]. The jet efflux spans the space between the two fins. The mainstream approach-lower surface, but they are displaced downwards by the fins to combine with the vortex sheet shed by the fins themselves. In consequence, the wide-spread suctions on the rear of the lower surface due to the vortices are reduced by the fins. This applies particularly outboard of the fins themselves, whereas the partial or total rearward extension of the fins as in arrangements (C) and (D), maintains high suctions between the fins rear of the fan duct. Fin (E) in Fig. 48, whose pressure distribution is shown in Fig. 49, is intermediate in size between fins (A) and (B) and the force measurements are correspondingly intermediate, except that there is no difference in the drag/lift ratio from (B). The tuft patterns suggested that the losses due to the separation on the outside of the fins might be responsible for extra drag so version (B) was modified to give local camber at the nose or 'toe-in', shown as (F) in Fig. 48b. There now appeared to be no separation at the fin leading-edge at any speed with the fan operating. The pressure distribution, Fig. 50, showed extra suctions in various places and the lift increment, Fig. 51, was less than (B) (and very nearly constant). The drag increment was still further reduced so that the drag/lift ratio was appreciably better than for (B). This is also true when the increments were measured above the bare wing, fan-off, datum and fin (F) is the best fin tested for this ratio, except above V_T/V_F of 0·5 where the bare wing or the full chord fin (D) score, mainly due to the large lift increments that these combinations yield.

The lift comparisons discussed so far are based on observations taken at selected forward speeds and fan rotational speeds. The influence of underfins on the flow through the fan was not included as the values of V_F were based on the appropriate measurements taken without the underfins. The pressure distributions of Figs. 49 and 50 show that the pressure between the fins immediately ahead of the fan is increased, but that the corresponding pressures *immediately* behind the fan are reduced by the presence of the fins at forward speeds. The mean pressure over the duct area appears to be increased, because inlet traverses taken at 40 ft/sec forward speed at 41·7 revs/sec fan rotational speed show that the flux through the fan duct is reduced by $3\frac{1}{2}$ per cent for fin (E) and by 5 per cent for fin (D) compared with the bare wing case: the mal-distribution at the inlet, however, is not affected by the presence of the fins. These flow reductions imply that the fan is working further up its characteristic (Fig. 20 of Ref. 2). From this information, and making the same assumptions as were used in deriving Fig. 22, the effect of fins (D) and (E) on the ideal output power ratio has been calculated for the conditions in which the traverses were taken. The effect is compared with the bare wing result in Fig. 52. On a power basis fin (E) shows little improvement over the bare wing, but arrangement (D) shows a substantial economy.

These measurements all suggest that for any future practical layout it ought to be possible to find an arrangement of underfins giving any required variation of lift with forward speed. In the present state of knowledge, wind-tunnel tests on the particular layout would be essential. Attempts to minimise the drag penalty could then be made by using fins with some thickness and a rounded leading-edge to cope with the movement of the local stagnation point with forward speed and with yaw, provided such artifices did not prejudice the arrangements for retracting the fins when not required.

There also appears to be no reason why such fins should not be equally applicable to jets emerging from fuselages and nacelles. Some such tests are reported in Refs. 13 and 14.

10. *Effects of other Devices,*

A number of other devices were also examined in an attempt to improve the flow conditions in the fan duct, but without a great deal of success. In several cases the failure to achieve a beneficial result was probably due to the crude nature of the actual device tested rather than to a failure of the basic principle involved. As a guide to other experimentors, however, a brief account of this phase of the work is given.

It was thought that the flow conditions generally would be improved by 'two-dimensionalising' the flow entering the fan duct. This was initially attempted by fitting a pair of fins of the shape 'A' in Fig. 53 on to the upper surface of the wing. These fins were 15 in. apart, greater than the duct diameter of 13·16 in., but the resulting corner between the fin and the outer edge of the inlet flare produced separation of the fin boundary-layer and consequent poor flow into the duct.

The circular bell-mouth in the upper surface of the wing was therefore replaced by a square inlet transition piece so that the fins could be mounted flush with its sides. In order to avoid the confusing effect of additional contraction, however, it was deemed desirable to make the square opening the same area as that of the circular duct. There proved to be inadequate duct inlet depth to accommodate the change of shape, as the overhang of the square opening in the middle of each side (Fig. 53) led to separation at zero forward speed, and the flow attached only in the corners. The patch of separated flow at the rear lip vanished at V_T/V_F of about 0·44, but the separations on the other three faces remained.

The square inlet was enlarged to reduce the overhang in the centre of the sides by one half. This reduced the extent of separated flow and lowered the wing speed at which separation at the rear of the entry was eliminated.

The addition of a 1 in. radius semi-circular bump with a small cambered slat to prevent boundary-layer separation, B, Fig. 53, gave a more uniform velocity distribution but failed to prevent under-turning of the flow at high forward speeds. This was cured at a forward speed ratio V_T/V_F of 0·24 by the addition of the substantial cambered vane 'C', but this proved not to be at the right setting for V_T/V_F equal to 0·44 for the flow separated from the upper surface of the vane in these conditions.

A further suggestion for turning the flow was based on the ideas of Ref. 16. A two-dimensional free-streamline slot perpendicular to the mainstream must be a step-down type of slot at all non-zero forward speeds. In such an entry the horizontal component of momentum of the air entering the slot is balanced by the forward pointing component of the reduced pressure acting on the exposed upstream lip. The entries produced by the bump, Fig. 53, 'D' and the tilted flap 'E' were intended to balance the momentum at V_T/V_F equal to 0·24. On the whole, this was so, the continuous bump producing steadier flow than the flap which the separated flow at its rear edge did not always meet the front lip of the duct satisfactorily. With both these devices, however, the flow through the fan was slightly reduced at a given fan rotational speed. In detail, too, the flows were not nearly as uniform as those discussed in Ref. 2 where a cascade of turning vanes produces a much better distribution of flow into the whole duct since the necessary pressure gradient is maintained between successive pairs of vanes without the static pressure deviating nearly so far from the mean.

It is concluded from the present and earlier tests that the most uniform flow into a fan unit arranged with its axis normal to the mainstream will be obtained with the use of relatively closely pitched cascades of refined design. A theoretical attack on this problem has been made and tests will be carried out in a special form of cascade tunnel which is more convenient for this purpose than the use of an actual fan-in-wing installation.

11. *Conclusions,*

It is shown that the increments in lift and drag and pitching moment due to the operation of a small fan installed at a forward position ($x/c = 0{\cdot}354$) in a large wing ($A_W/A_F = 44$) vary considerably with

forward speed. The results can be correlated by expressing the force increments in terms of the momentum flux and the forward speed in terms of mean flow speed through the fan, but the variations are not explicable on the basis of a simple momentum argument. It is concluded that the lift is affected by jet-efflux/mainstream interactions and in addition by local changes in circulation, but these effects are not investigated here.

The earlier analysis in Ref. 2 of the flow through the fan, which was mainly concerned with flow maldistribution, has been extended: the variation with forward speed of the total head rise demanded of the fan has been related to static pressure changes at the fan duct on both upper and lower surfaces. Lower surface suctions are present between static conditions and a forward speed ratio V_T/V_F of 0·88. Above this speed the pressure difference is of opposite sign, a feature that, without modification of the exit, inhibits autorotation for flight starting of the fan.

It is interesting that at constant fan rotational speed the 'net standard thrust' is nearly constant from static conditions up to a forward speed ratio V_T/V_F of 0·88. The increase in momentum flux due to the fan progressing down its characteristic with increase of forward speed is exactly counterbalanced by the lower surface suctions that induce the extra flow, but it is shown that this is fortuitous.The reduction in overall lift as far as V_T/V_F equal to 0·3 and subsequent rise are therefore, in this particular case, wholly associated with the undersurface suctions acting on the wing outside the duct region. At V_T/V_F equal to 0·8, the momentum flux exceeds $\rho A_F(\overline{V}_F)^2$ by 14 per cent on account of the maldistribution and this margin rises steeply with further increase in V_T/V_F.

Apart from the effect of rotation of the fan thrust vector, change of incidence has only significant effects on the force increments due to the fan at values of V_T/V_F greater than 0·5, under which conditions the magnitude of the force increments are not of great importance as transition to wing-borne flight is largely complete.

The effects of plain and split flap deflection are presented. Above about 15 deg flap deflection, the lift increments due to fan operation at high forward speeds are greatly reduced, and with 30 deg flap deflection became negative. This is due to the jet efflux or the entrained flow impinging on to the deflected flap. Associated with some movements of the position of flow separation on the lower surface of the flap there is a limited range of control reversal (for plain flap deflections between 20 deg and 30 deg at forward speeds $0{\cdot}4 < V_T/V_F < 0{\cdot}8$ or $0{\cdot}25 < \mu < 0{\cdot}5$). It is concluded that it would be unwise to fit trailing-edge controls immediately downstream of a lifting fan.

An exit cascade is effective in turning the efflux but the large accompanying losses in lift are thought to be due to a Reynolds number effect which would not be so bad at full scale. The results on lift and drag changes are presented in a form that shows an economy in power requirements only up to 20 deg jet deflection.

Underfins fitted tangentially to the duct exit on the lower surface can be used to modify the forward speed lift characteristics of the fan wing at constant fan rotational speed. The lift droop can be eliminated or a rising characteristic obtained by a suitable size and disposition of fins. The principal effect is to reduce the strength of the undersurface interactions by increasing the distance between the wing lower surface and the trailing vortices in the jet plume, which with fins present spring from the lowest edge of the fin. Although the pressure rise across the fan is increased slightly so that the mass flow is reduced by up to 5 per cent, a substantial power economy is possible.

More uniform flow into the fan unit had been obtained with closely pitched cascades[2] than with other devices here tested. However, improved designs of cascade could be more easily tested on a rig specifically intended for this purpose than on a model fan-in-wing installation. Such a rig is being constructed.

NOTATION

ρ	Density
A_F	Fan annulus area
A_W	Wing area
c	Wing chord
d	Fan diameter
r	Radial distance from fan axis
x	Chordwise distance from wing leading edge
z	Spanwise distance from centre line
n	Fan rotational speed, revs/sec
V_T	Forward speed
V_F	Mean axial speed of flow through fan (approximately 0·94 $V_{F\,\mathrm{nom}}$ for 13·16 in. diameter fan)
$V_{F_{\mathrm{nom}}}$	Mean axial speed of flow through fan as evaluated from downstream traverses
μ	Advance ratio, $= V_T/\pi nd \quad = \pi nd\sqrt{(\frac{1}{2}\rho A_F/L)}$
$1/\sqrt{C_T}$	Fan speed parameter $\quad = V_T\sqrt{(\frac{1}{2}\rho A_W/L)}$
$1/\sqrt{C_L}$	Forward speed parameter
L	Lift
D	Drag
M	Pitching moment
p	Static pressure
p_T	Undisturbed static pressure
H	Total head
H_D	Undisturbed total head
C_p	Pressure coefficient $= (p-p_T)/\frac{1}{2}\rho V_T^2$
C_p'	$= C_p V_T^2/V_F^2$
C_L, C_D, $C_{Mc/4}$	Lift, drag and pitching moment coefficients
Δ	Increments in above due to opening fan aperture and running fan
Δ	(In Figs. 4 and 25 only) increments in above due to opening fan aperture only
Suffix $_0$	Zero speed value
K_p	Ideal fan output power coefficient } See section 3
ξ	Ideal output power ratio }
α	Incidence
β	Exit cascade vane angle to lower surface
η	Flap deflection
θ	Angular position about fan axis

REFERENCES

No.	*Author(s)*	*Title, etc.*
1	N. Gregory	On the representation of fan-wing characteristics in a form suitable for the analysis of transition motions, with results of tests of an aspect ratio—1 wing with fan at 0·354 chord. A.R.C. C.P. 552, August 1959.
2	N. Gregory, W. G. Raymer Edna M. Love	The effect of forward speed on the inlet flow distribution and performance of a lifting fan installed in a wing. A.R.C. R. and M. 3388. June, 1962.
3	N. Gregory and W. G. Raymer	Wind tunnel tests on the Boulton Paul rectangular wing (aspect ratio 2) with lifting fan – Series I. A.R.C.20 356, August, 1958.
4	N. Gregory and W. G. Raymer	Wing tunnel tests on the Boulton Paul rectangular wing (aspect ratio 2) with lifting fan – Series II. A.R.C.21 127, July, 1959.
5	N. Gregory and W. G. Raymer	Wind tunnel tests on the effects of the apex fan on a swept wing project for V.T.O.L. with three lifting fans. A.R.C.21 260, September, 1959.
6	L. A. Wyatt	Preliminary note on wind-tunnel tests of a wing fitted with multiple lifting-fans. A.R.C.21 377, October, 1959.
7	—	Report of the Definitions Panel on the definitions of the thrust of a jet engine and of the internal drag of a ducted body. A.R.C. C.P. 190. May, 1954.
8	ed. B. Thwaites	*Incompressible Aerodynamics.* 1960. (Fig. VIII.28). Oxford Univ. Press.
9	—	A note on the aerodynamics of a wing-fan system. Boulton Paul Aircraft Tech. Note No. 2. A.R.C.19 890, February, 1958.
10	L. J. S. Bradbury and.. M. N. Wood ..	The static pressure distribution around a circular jet exhausting normally from a plane wall into an airstream. A.R.C. C.P.822, August, 1964.
11	R. D. Vogler	Surface pressure distributions induced on a flat plate by a cold air jet issuing perpendicularly from the plate and normal to a low-speed free-stream flow. NASA TN D–1629, March, 1963.
12	S.-A. Norland..	An investigation of the lift produced by a fan in a two-dimensional wing. *J. Am. Helicopter Soc.* Vol. 7 No. 4 pp.25 to 32, October, 1962.
13	W. J. G. Trebble and J. E. Hackett	Low-speed wind-tunnel tests on a streamlined body containing a ducted lifting fan. A.R.C.25 084, May, 1963.

14 J. E. Hackett .. .. .. Wind-tunnel tests on an aircraft model fitted with a lifting fan unit installed in the body.
Ph.D. Thesis, University of London. March, 1964.

15 L. A. Wyatt .. .. .. Private communication.

16 E. J. Watson .. .. .. Free streamline suction slots.
A.R.C. R. and M.2177. February, 1946.

APPENDIX

Brief Comparisons between the N.P.L. Wind-Tunnel Tests of Wings fitted with Single Lifting Fans

The planforms and leading dimensions of the three lifting-fan wings tested at N.P.L. are shown in Fig. 54. The variations with forward speed of the lift and drag increments at zero incidence due to fan operation on these wings are shown, plotted non-dimensionally, in Figs. 55 and 56. The corresponding curves for the variation of the chordwise position at which the lift increment due to the fan acts are given in Fig. 57. The curves for the aspect ratio 2 wing marked 'different fan' refer to a fan whose axial flow component increases with radius to a maximum near the tips. The other fans have a more uniform distribution. The effect of high velocity air near the outside of the efflux is to enhance the mixing processes between jet efflux and mainstream. Consequently the fall-off in lift at low forward speeds and the pitch-up moment are more severe than with the fan with more uniform flow.

Study of these three figures shows that the fall-off in lift at low forward speeds (compared with the static value) is associated with a forward fan position and a larger value of A_W/A_F. The steep rise in lift at higher forward speeds is correspondingly enhanced (in the case of the rectangular wings) by a rearward fan location. The drag increments are large and in the range of 20 per cent to 50 per cent in excess of the sink drag of the air entering the fan. The exception to this is the case of the swept arrowhead wing tested with its apex pointing forward. In this configuration the reduction in drag increment would appear to be due to the extreme forward location of the fan so that regions close to the fan inlet experiencing low pressures due to the inflow have a forward facing component. This also shows in the negative and positive non-zero values of drag obtained, apex forward and tail-first respectively, at zero forward speed.

The most forward position of the centre of pressure of the lift increment also increases with a more forward fan location and with large values of A_W/A_F. It is least for the swept arrowhead wing tested tail first where there was little surface to the rear of the fan, but this configuration was also the worst for lift increment.

TABLE 1

Fan blading design and performance specification

Free vortex design

	$2r/d$	α_1	α_2	ε	$(S/c)_N$	$(S/c)_A$	α_1'	α_2'	θ	ξ	δ	c	N
Rotor	1·0	59·2	52·4	6·8	3·2	1·57	59·2	48·2	11·0	53·7	4·2	1·25	
	0·75	51·5	37·0	14·5	1·42	1·18	51·5	30·2	21·3	40·85	6·8	1·25	21
	0·50	40	4·7	35·3	0·71	0·78	40	−4·7	44·7	17·65	9·4	1·25	
Stator	1·0	20·7	0	20·7	2·4	1·65	20·7	−8·3	29·0	6·2	8·3	1·25	
	0·75	26·7	0	26·7	1·53	1·24	26·7	−8·9	35·6	8·9	8·9	1·25	20
	0·50	37·1	0	37·1	0·77	0·82	37·1	−10·2	47·3	13·45	10·2	1·25	

C.4 Circular arc aerofoils

Inlet guide vanes with zero camber and outlet engles

Mean air speed	85·5 ft/sec
Thrust	12·3 lb
Fan speed	41·7 rev/sec
Mass flow	4·64 lb/sec
Fan adiabatic efficiency	0·80
Gear efficiency	0·80
Motor speed	125 rev/sec
Motor power	1·5 b.h.p.

Notation for Table 1 only

r Radius
d Fan diameter
α_1 Air inlet angle
α_2 Air outlet angle
$\varepsilon = \alpha_1 - \alpha_2$, deflection
α_1' Blade inlet angle
α_2' Blade outlet angle
$\theta = \alpha_1' - \alpha_2'$, camber
ξ Stagger angle
$\delta = \alpha_2 - \alpha_2'$, deviation
N number of blades
S gap
c chord, in.
Suffix N nominal
Suffix A actual

TABLE 2

Lift, Drag and Pitching Moments for the Plain Wing in Duplex Wind Tunnel

—12° *Incidence*

Fan Condition	Windspeed V_T ft/sec	Lift lb	Drag lb	Pitching Moment ft lb	
				$\frac{1}{4}$ Chord	Fan Axis
Aperture Sealed	0				
	20	—5·6	0·93	—2·17	—4·39
	25	—9·1	1·48	—3·48	—7·09
	30	—13·0	2·12	—4·89	—10·05
	40	—22·9	3·76	—8·74	—17·83
	50	—36·5	6·04	—13·14	—27·61
Aperture open	0				
	20	—4·8	1·00	—1·53	—3·38
	25	—7·9	1·61	—2·41	—5·47
	30	—11·2	2·31	—3·57	—7·90
	40	—21·1	4·23	—5·95	—14·13
	50	—33·7	6·90	—9·13	—22·16
Fan running at 41·7 rev/sec	0	9·1	—1·86	—5·54	—2·02
	20	2·5	3·01	5·93	7·78
	25	—1·2	5·04	11·80	12·54
	30	—4·6	6·99	16·96	16·70
	40	—11·3	11·71	27·93	25·92
	50	—17·4	15·78	31·29	27·63

—8° *Incidence*

Aperture sealed	0				
	20	—3·7	0·56	—1·71	—3·31
	25	—5·8	0·88	—3·03	—5·54
	30	—8·3	1·25	—4·31	—7·90
	40	—14·7	2·22	—7·78	—14·13
	50	—23·1	3·46	—14·27	—22·23
Aperture open	0				
	20	—3·1	0·58	—1·46	—2·77
	25	—5·1	0·97	—2·45	—4·60
	30	—7·5	1·45	—3·60	—6·75
	40	—13·3	2·56	—6·59	—12·18
	50	—21·4	4·09	—10·27	—19·28
Fan running at 41·7 rev/sec	0	9·3	—1·44	—5·49	—1·48
	20	4·5	3·17	6·83	9·86
	25	2·1	4·79	12·81	15·16
	30	—0·1	6·56	19·86	20·26
	40	—3·0	10·59	29·19	30·76
	50	—5·0	14·17	33·45	35·09

TABLE 2—(contd.)

—4° *Incidence*

Fan Condition	Windspeed V_T ft/sec	Lift lb	Drag lb	Pitching Moment ft lb	
				$\frac{1}{4}$ Chord	Fan Axis
Aperture sealed	0				
	20	—1·7	0·36	—1·15	—1·90
	25	—2·7	0·54	—1·78	—2·99
	30	—3·9	0·76	—2·29	—4·20
	40	—7·1	1·37	—4·08	—7·61
	50	—11·3	2·17	—6·94	—12·02
Aperture open	0				
	20	—1·5	0·37	—1·18	—1·83
	25	—2·3	0·60	—1·87	—2·85
	30	—3·4	0·87	—2·61	—4·07
	35	—5·0	1·23	—3·24	—5·41
	40	—6·6	1·62	—4·09	—6·94
	50	—10·4	2·62	—6·44	—10·88
Fan running at 41·7 rev/sec	0	9·4	—0·79	—5·51	—0·54
	20	6·6	3·23	6·67	11·06
	25	4·9	4·23	12·19	16·03
	30	4·1	6·07	18·66	22·68
	35	3·1	8·16	26·98	31·15
	40	4·1	9·84	31·33	36·54
	50	5·1	13·36	38·67	45·51

0° *Incidence*

Aperture sealed	0				
	6·8	0	0·04	—0·01	0·01
	13·3	0	0·11	—0·13	—0·09
	20	—0·05	0·27	0·09	0·10
	25	—0·05	0·43	0·03	0·09
	30	—0·1	0·66	0·04	0·22
	40	—0·15	1·12	0·18	0·49
	50	—0·2	1·80	0·25	0·78
Aperture open	0				
	20	0	0·36	0·18	0·31
	25	0·05	0·59	0·19	0·43
	30	0·15	0·82	0·26	0·63
	35	0	1·10	0·30	0·69
	40	0·25	1·40		0·96
	50	0·45	2·20	0·70	1·72
				0·33	
Fan running at 21·7 rev/sec	55	4·8	6·59	18·32	23·23
	60	4·0	5·75	11·28	15·46

TABLE 2—(contd.)

0° *Incidence*—(contd.)

Fan Condition	Windspeed V_T ft/sec	Lift lb	Drag lb	Pitching Moment ft lb	
				¼ Chord	Fan Axis
Fan running at 23·3 rev/sec	0	2·7	—0·04	—1·25	0·20
	7·0	2·8	0·67	—0·13	1·62
	13·7	2·1	1·48	4·02	5·68
	20	2·4	2·55	9·41	11·61
	25	3·6	3·63	12·25	15·49
	30	5·2	4·43	14·06	18·45
	35	6·4	5·37	16·37	21·74
	40	7·5, 7·0	6·08	19·03, 19·30	25.25
	45	7·5	6·81	21·20	27·68
	50	5·7	7·04	23·66	29·24
	55	5·1	7·54	25·53	30·96
	60	5·4	7·54	21·35	26·95
Fan running at 26·7 rev/sec	0	3·6	—0·06	—1·66	0·27
	7·0	3·7	0·76	—0·85	1·42
	13·7	3·1	1·67	3·41	5·68
	20	2·9	2·68	9·49	12·01
	25	3·2	3·84	14·42	17·51
	30	5·1	4·93	17·17	21·33
	35	6·7	6·00	19·22	24·97
	40	8·4	6·97	21·59	28·61
	45	8·8	7·89	25·57	33·13
	50	8·2	8·60	30·22	37·71
	55	7·7	9·11	32·29	39·69
Fan running at 30 rev/sec	0	4·9	—0·10	—2·35	0·27
	7·0	4·8	0·90	—1·43	1·49
	13·7	4·0	1·88	2·30	5·68
	20	3·5	2·90	9·83	12·75
	25	3·8	4·07	14·95	18·45
	30	6·1	5·44	18·59	23·82
	35	7·1	6·52	22·03	28·19
	40	8·8	7·66	25·36	32·84
	45	10·5	8·87	28·60	37·43
	50	11·0	9·94	32·87	42·35
	55	11·0	11·09	38·94	48·83
	60	10·7	11·88	41·94	51·95
Fan running at 35 rev/sec	0	6·7	—0·20	—2·96	0·60
	7·0	6·5	1·09	—2·21	1·69
	13·7	5·9	2·12	1·73	5·68
	20	5·1	3·33	9·88	13·82
	25	4·9	4·51	15·74	19·99
	30	5·3	5·89	21·89	26·85
	35	8·2	7·52	25·72	32·83
	40	9·8	8·84	29·71	38·15
	50	12·7	11·43	38·14	49·07
	55	14·4	13·01	44·95	57·36
	60	15·2	14·25	49·76	63·04

TABLE 2—(contd.)

0° *Incidence*—(contd.)

Fan Condition	Windspeed V_T ft/sec	Lift lb	Drag lb	Pitching Moment ft lb	
				¼ Chord	Fan Axis
Fan running at 41·7 rev/sec	0	9·6	—0·17	—4·47	0·67
	7·0	9·3	1·29	—3·34	2·16
	13·6	8·9	2·45	—0·14	5·55
	20	8·3	3·92	9·07	14·96
	25	7·4	5·21	16·01	21·87
	30	6·9	6·58	23·32	29·39
	35	7·9	8·10	30·43	37·58
	40	11·4	10·30	36·36	46·18
	50	15·2	13·27	46·37	59·31
	60	18·2	16·30	55·88	71·51

4° *Incidence*

Aperture sealed	0				
	20	1·9	0·38	1·23	2·47
	25	2·8	0·62	2·16	4·00
	30	4·0	0·84	3·00	5·61
	40	7·2	1·51	5·22	9·92
	50	11·4	2·36	7·96	15·40
Aperture open	0				
	20	1·6	0·41	1·20	2·27
	25	2·6	0·68	2·05	3·80
	30	3·8	0·99	2·71	5·27
	35	5·4	1·32	3·89	7·49
	40	6·7	1·68	4·90	9·39
	50	10·6	2·63	7·50	14·59
Fan running at 41·7 rev/sec	0	9·3	0·55	—3·78	1·75
	20	9·9	4·43	9·66	17·05
	25	10·1	5·51	17·04	24·97
	30	11·0	6·86	24·25	33·23
	35	12·7	8·29	33·27	43·78
	40	17·6	10·63	38·77	53·00
	50	24·5	13·81	50·82	70·24

8° *Incidence*

Aperture sealed	0				
	6·9	0·45	0·08	0	0·55
	13·4	1·65	0·27	0·09	1·26
	20	3·6	0·59	1·67	4·08
	25	5·7	0·94	2·67	6·49
	30	8·3	1·35	4·63	10·18
	40	14·7	2·44	7·94	17·79
	50	23·2	3·82	12·97	28·50

TABLE 2—(contd.)

8° *Incidence*—(contd.)

Fan Condition	Windspeed V_T ft/sec	Lift lb	Drag lb	Pitching Moment ft lb	
				¼ Chord	Fan Axis
Aperture open	0				
	20	3·4	0·67	1·62	3·94
	25	5·4	1·05	2·87	6·55
	30	7·8	1·54	4·18	9·51
	40	14·0	2·69	7·31	16·85
	50	22·3	4·31	11·08	26·29
Fan running at 23·3 rev/sec	0	2·7	0·36	—1·03	0·74
	6·9	3·3	1·10	—0·68	2·29
	13·2	3·9	1·70	4·78	7·85
	20	5·8	2·81	10·21	14·90
	25	8·6	3·96	14·01	20·87
	30	11·8	4·97	17·43	26·64
	35	15·9	6·13	21·80	33·97
	40	20·1	7·39	25·74	40·97
	45	25·1	8·21	27·26	45·83
	50	27·4	7·80	26·74	46·51
	55	32·6	8·15	21·23	44·26
Fan running at 30 rev/sec	0	4·6	0·61	—2·01	1·01
	7·4	5·4	1·75	—1·23	2·76
	12·8	5·9	2·39	3·83	8·40
	20	7·1	3·47	11·30	17·05
	25	9·1	4·56	16·81	24·23
	30	13·0	6·01	21·30	31·68
	35	16·9	7·40	26·63	39·95
	40	21·8	8·94	31·78	48·70
	50	32·3	11·92	42·25	66·74
Fan running at 35 rev/sec	0	6·3	0·81	—2·51	1·61
	7·7	7·4	2·01	—1·81	3·49
	12·8	7·7	2·90	2·34	8·20
	20	8·9	4·05	11·11	18·19
	25	10·7	5·05	17·05	25·64
	30	13·2	6·34	22·98	33·63
	35	18·3	8·39	28·80	43·38
	40	22·9	10·00	35·24	53·27
	50	43·2	13·34	46·82	73·06
Fan running at 41·7 rev/sec	0	9·2	1·08	—3·42	2·55
	8·6	10·1	3·07	—2·76	4·61
	12·3	10·8	3·74	0·48	8·56
	20	12·0	5·04	10·31	19·67
	25	13·4	6·24	17·20	27·92
	30	15·4	7·58	25·77	38·27
	40	22·2	10·80	42·16	60·12
	50	35·5	15·27	53·93	81·79

TABLE 2—(contd.)

12° *Incidence*

Fan Condition	Windspeed V_T ft/sec	Lift lb	Drag lb	Pitching Moment ft lb	
				$\frac{1}{4}$ Chord	Fan Axis
Aperture sealed	0				
	20	5·6	0·99	2·15	6·10
	25	9·0	1·59	3·90	10·25
	30	12·8	2·29	5·50	14·55
	40	22·7	4·02	9·75	25·78
	50	36·1	6·50	21·68	47·23
Aperture open	0				
	20	5·3	1·12	1·46	5·29
	25	8·1	1·71	2·45	8·30
	30	11·8	2·47	3·61	12·13
	40	21·7	4·58	7·89	23·57
	50	34·2	7·20	12·47	37·17
Fan running at 41·7 rev/sec	0	9·1	1·67	—3·44	3·02
	20	14·0	5·98	8·79	20·34
	25	16·4	7·14	16·07	29·67
	30	20·0	8·54	23·98	40·49
	40	29·6	12·10	40·52	64·69
	50	45·9	17·26	53·36	90·13

TABLE 3

Analysis of Fan Traverse Measurements at Zero Incidence

Forward speed, V_T ft/sec	0	14·3	20	30	40	50	71·4[a]	89·4[a]
Fan rotational speed, rev/sec	41·7	41·7	41·7	41·7	41·7	41.7	41·7[a]	41·7[a]
Mean airspeed from inlet traverse, ft/sec	83·9	87·5		90·0	91·4	90·9	(81·3)[b]	(67·0)[b]
Standard deviation, σ	0·09	0·09		0·15	0·19	0·22		
Mean speed from stator traverse, ft/sec	89·8		94·6	96·0	95·8	96·4	86·2	71·0
Standard deviation, σ	0·16		0·14	0·14	0·15	0·18	0·38	0·60
V_T/V_F	0	0·16	0·22	0·33	0·44	0·55	0·88	1·33
Momentum flux at stators, $\rho A_F \overline{V_F^2}$, lb	12·02	13·20	13·90	14·36	14·52	14·48	12·92	10·43
$\int (p_2 - p_0) dA$ at stators across annulus, lb	—1·24		—2·37	—2·77	—2·70	—2·82	—1·94	—0·83
$\int (p_2 - p_0) dA$ at stators across hub, lb	—0·54		—0·96	—1·13	—1·04	—1·07	—0·79	—0·35
Net standard traverse thrust, lbs (sum of previous three rows)	10·24		10·57	10·46	10·78	10·59	10·20	9·25
(1) Measured lift on whole wing, lb	9·65		8·35	7·0	11·55	15·4	24·4	18·8
Difference, additional lift[c] experienced by surrounding wing, induced by tunnel constraint and circulation changes, lb	—0·59		—2·22	—3·46	+0·77	4·81	14·2	9·55
(3) Blade load, from pressure rise across fan, lb	5·68		5·04	4·40	3·86	3·16	1·24	—1·62
(2) Difference from measured lift, pressure force on wing and hub, lb	3·97		3·31	2·60	7·69	12·24	23·1	20·4
$C_p' = \frac{H_m - H_D/\frac{1}{2}\rho V_F^2}{p - p_T/\frac{1}{2}\rho V_F^2}$ at inlet traverse plane	—0·005	—0·002		—0·015	—0·02	—0·06		
	—1·00	—1·00		—1·00	—0·98	—0·94		
$C_p' = \frac{H_m - H_D/\frac{1}{2}\rho V_F^2}{p - p_T/\frac{1}{2}\rho V_F^2}$ at stator traverse plane	1·02		0·73	0·66	0·57	0·47	0·26	—0·41
	—0·20		—0·35	—0·42	—0·39	—0·40	—0·35	—0·22

NOTES: (a) These two columns are scaled up (at constant values of V_T/V_F) from measurements at 40 and 50 ft/sec forward speed with 23·3 rev/sec.

(b) These speeds could not be obtained from the traverse as the yawmeter calibration was exceeded. The same factor, 0·94 on exit velocity was taken as held at lower values of V_T/V_F.

(c) Includes post-exit thrust.

TABLE 4

Lift, Drag and Pitching Moments for Wing with Plain Flap in Duplex Wind Tunnel

Flap +15° (*T.E. down*) 0° *Incidence*

Fan Condition	Windspeed V_T ft/sec	Lift lb	Drag lb	Pitching Moment ft lb	
				¼ Chord	Fan Axis
Aperture sealed	0				
	13·5	1·4	0·26	—2·38	—1·53
	20	3·1	0·56	—5·86	—3·98
	25	4·9	0·91	—9·39	—6·41
	30	6·9	1·32	—13·65	—9·44
	40	12·3	2·34	—23·77	—16·28
	50	19·5	3·71	—37·81	—25·93
Fan running at 41·7 rev/sec	0	9·4	—0·26	—4·60	0·40
	12·1	10·7	2·25	—3·76	2·84
	20	11·7	4·07	1·00	8·78
	25	12·9	5·50	3·53	12·47
	30	14·9	7·00	6·22	16·77
	40	24·2	11·21	7·83	24·91
	50	34·3	15·09	3·57	27·50

Flap +15° 8° *Incidence*

Aperture sealed	50	45·2	9·69		
Fan running at 41·7 rev/sec	50	58·5	21·71		

Flap —15° 0° *Incidence*

Aperture sealed	0				
	13·2	—1·4	0·27	2·73	2·07
	20	—3·1	0·53	5·37	3·88
	25	—4·8	0·90	8·36	6·08
	30	—6·8	1·27	12·01	8·77
	40	—12·1	2·30	22·92	17·18
	50	—19·0	3·58	37·47	28·44
Fan running at 41·7 rev/sec	0	9·5	—0·07	—4·45	0·67
	12·3	7·5	2·27	2·47	7·34
	20	4·9	3·96	13·86	17·92
	25	2·6	3·84	23·94	26·71
	30	0·3	4·97	34·06	35·98
	40	—0·6	11·23	60·23	63·88
	50	—2·8	14·83	84·25	87·98

TABLE 5

Lift, Drag and Pitching Moments for Wing with Split Flap in Duplex Wind Tunnel

Split Flap 30° —8° *Incidence*

Fan Condition	Windspeed V_T ft/sec	Lift lb	Drag lb	Pitching Moment ft lb	
				$\frac{1}{4}$ Chord	Fan Axis
Aperture sealed	50	5·2	6·39		
Fan running at 41·7 rev/sec	50	7·6	14·16		

Split Flap 30° —4° *Incidence*

Aperture sealed	0				
	20	2·9	1·15	—11·07	—7·28
	25	4·4	1·81	—14·68	—11·86
	30	6·2	2·41	—20·43	—16·50
	40	12·0	4·97	—38·23	—30·53
	50	19·3	8·07	—61·11	—48·71
Fan running at 41·7 rev/sec	0	9·3	—0·76	—5·17	—0·67
	20	10·1	3·80	—0·60	5·76
	25	10·4	5·07	0·18	7·09
	30	11·5	6·79	1·69	9·71
	40	14·4	10·88	6·19	16·98
	50	18·9	14·89	2·25	16·61

Split Flap 30° 0° *Incidence*

Aperture sealed	0				
	13·1	2·2	0·74	—3·67	—2·22
	20	4·7	1·54	—8·69	—5·60
	25	7·4	2·35	—13·27	—8·43
	30	11·1	3·71	—19·60	—12·27
	40	19·8	6·67	—36·09	—23·00
	50	31·6	10·79	—57·56	—36·61
Fan running at 23·3 rev/sec	0	2·8	—0·07	—1·42	0·07
	20	5·7	3·23	0·99	5·22
	25	7·5	4·35	1·63	7·23
	30	10·0	5·62	0·62	8·03
	40	17·3	8·77	—7·93	4·55
	50	26·9	12·61	—22·72	—3·68

TABLE 5—(contd.)

Split Flap 30° 0° *Incidence*—(contd.)

Fan running at 30 rev/sec	0	4·7	—0·07	—2·47	0·05
	20	7·3	3·80	0·39	5·69
	25	9·3	5·17	1·10⁻	7·97
	30	11·3	6·54	1·81	10·25
	40	18·0	10·01	0·25	13·55
	50	27·7	14·30	—7·18	9·35
Fan running at 41·7 rev/sec	0	9·2	—0·19	—4·38	0·54
	12·9	10·6	2·68	—3·26	3·43
	20	11·9	4·76	—0·15	7·98
	25	13·6	6·46	0·79	10·45
	30	15·7	8·38	2·06	13·54
	40	21·4	12·23	8·24	24·17
	50	30·1	16·94	3·98	26·29

Split Flap 30° 4° *Incidence*

Aperture sealed	0				
	20	6·8	2·19	—7·92	—3·18
	25	10·6	3·48	—13·03	—5·61
	30	15·7	5·21	—18·97	—7·96
	40	28·6	9·44	—34·98	—14·94
	50	44·9	14·86	—55·53	—24·05
Fan running at 41·7 rev/sec	0	9·1	0·47	—3·90	1·48
	20	14·1	5·69	0·31	10·60
	25	17·2	7·91	0·88	13·81
	30	20·6	10·03	3·15	18·85
	40	28·7	14·22	9·25	31·23
	50	41·9	19·98	5·73	37·51

Split Flap 60° 0° *Incidence*

Aperture sealed	0				
	12·4	3·3	1·69	—5·67	—3·28
	20	8·3	4·31	—14·17	—8·15
	25	13·3	6·90	—22·25	—12·60
	30	19·2	10·08	—31·41	—17·44
	40	34·3	17·64	—56·71	—31·87
	50	54·8	28·06	—89·15	—49·52
Fan running at 41·7 rev/sec	0	9·1	—0·16	—4·34	0·54
	12·95	12·4	3·72		
	20	15·7	7·15	—5·79	4·21
	25	19·1	10·36	—9·15	4·87
	30	23·6	13·93	—13·32	4·40
	35	29·5	17·87		
	40	35·7	21·96	—23·92	3·20
	45	43·6	26·70		
	50	52·4	31·77	—38·23	1·42

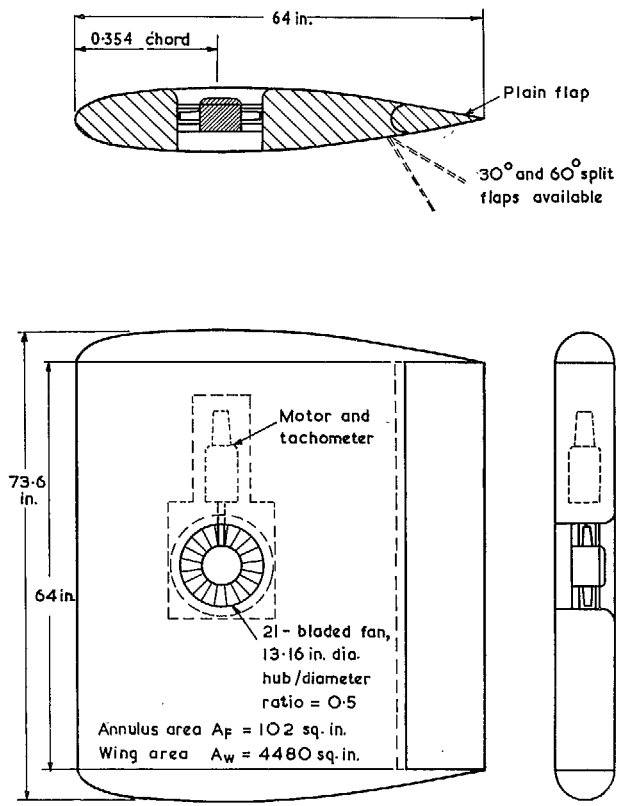

FIG. 1. General arrangement of model.

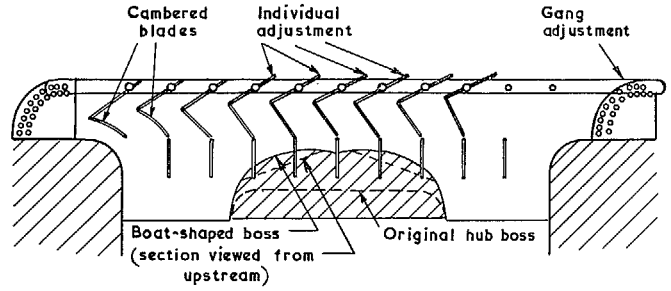

(a) Adjustable intake cascade, viewed from side.

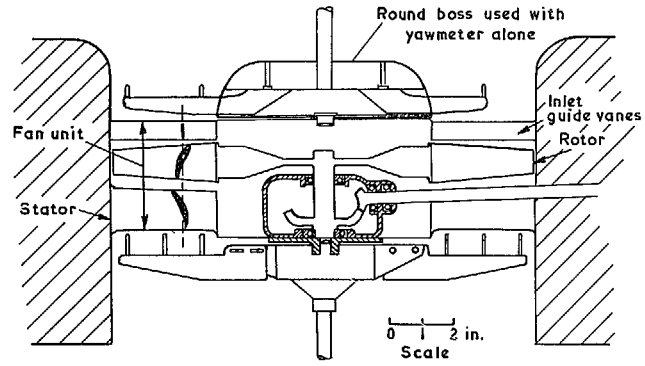

(b) Fan unit showing inlet guide vanes, rotor, stator, gear box and driving shaft, with the (alternative) upstream and downstream yawmeter rakes (viewed from downstream).

FIG. 2. Details of installation of fan unit, intake cascade and yawmeter rakes.

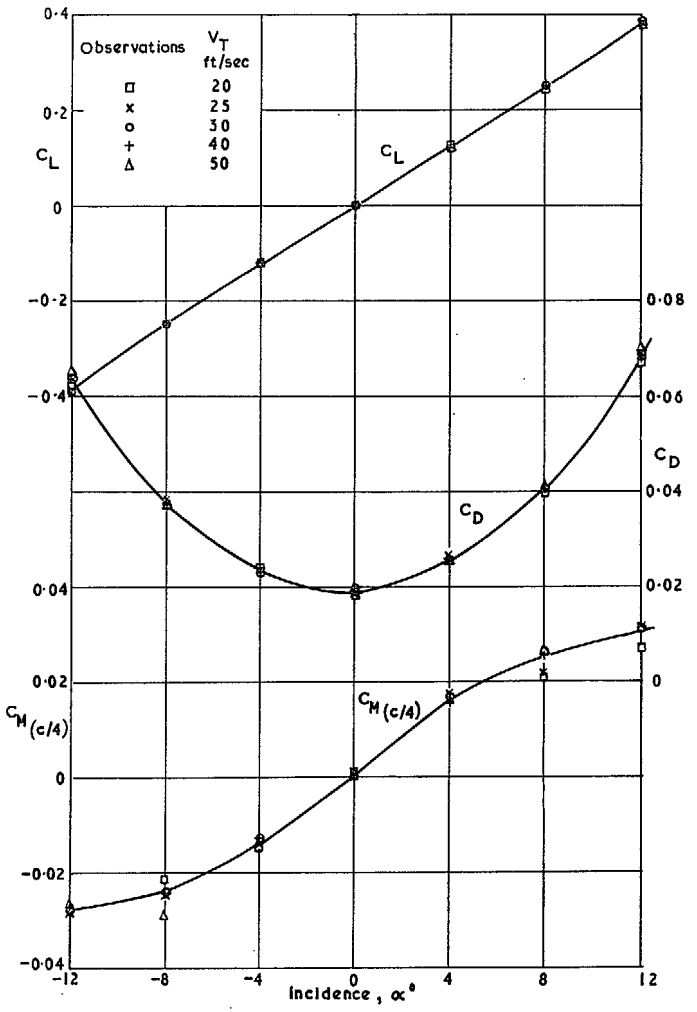

FIG. 3. Variation of C_L, C_D and $C_{M(c/4)}$ with incidence α. Fan duct sealed.

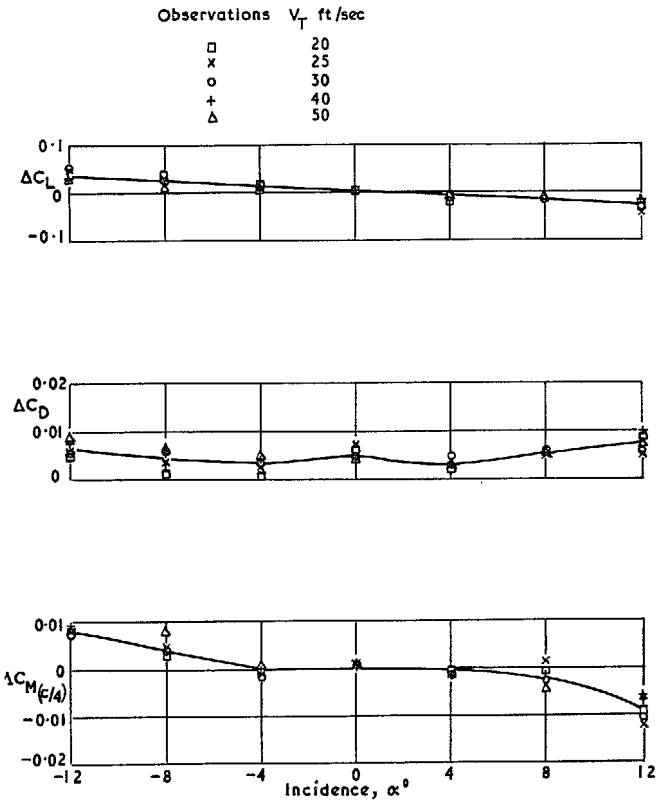

FIG. 4. Increments in C_L, C_D and $C_{M(c/4)}$ obtained by opening fan aperture [e.g. C_L gap open = C_L gap sealed (Fig. 3) + ΔC_L]

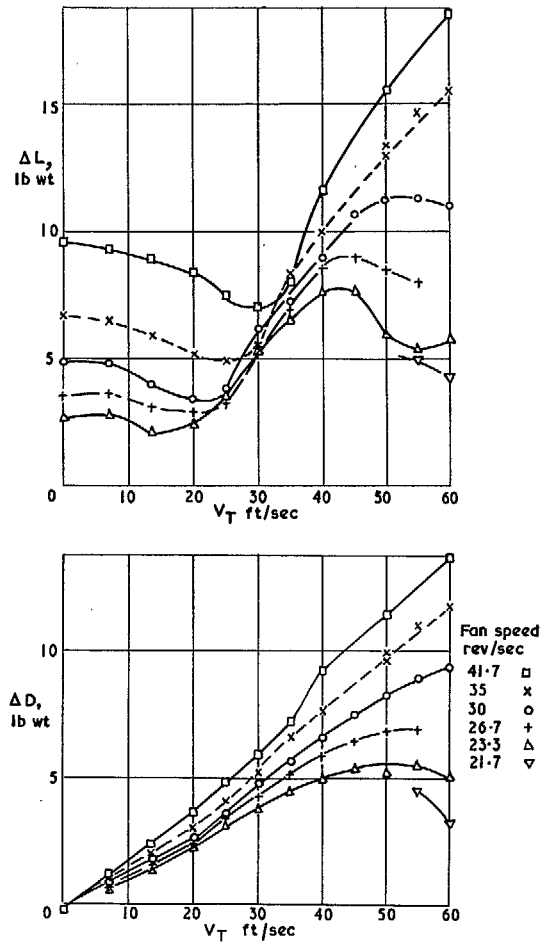

FIG. 5. Variation with forward speed of the lift and drag increments due to the fan, at zero wing incidence.

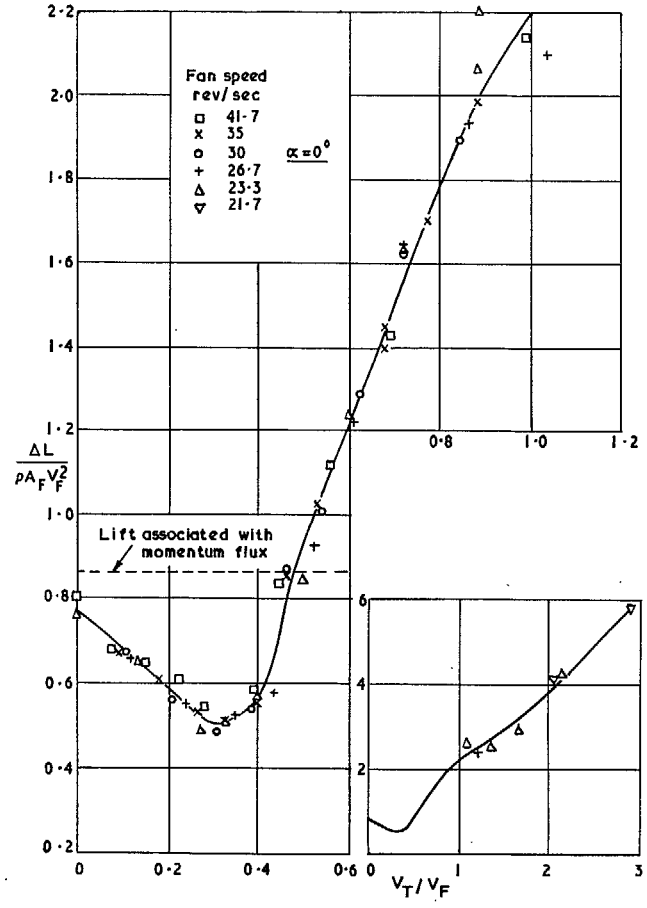

FIG. 6. Variation with forward speed ratio of the lift increment due to the fan, measured as a proportion of the momentum flux through the fan, at zero wing incidence.

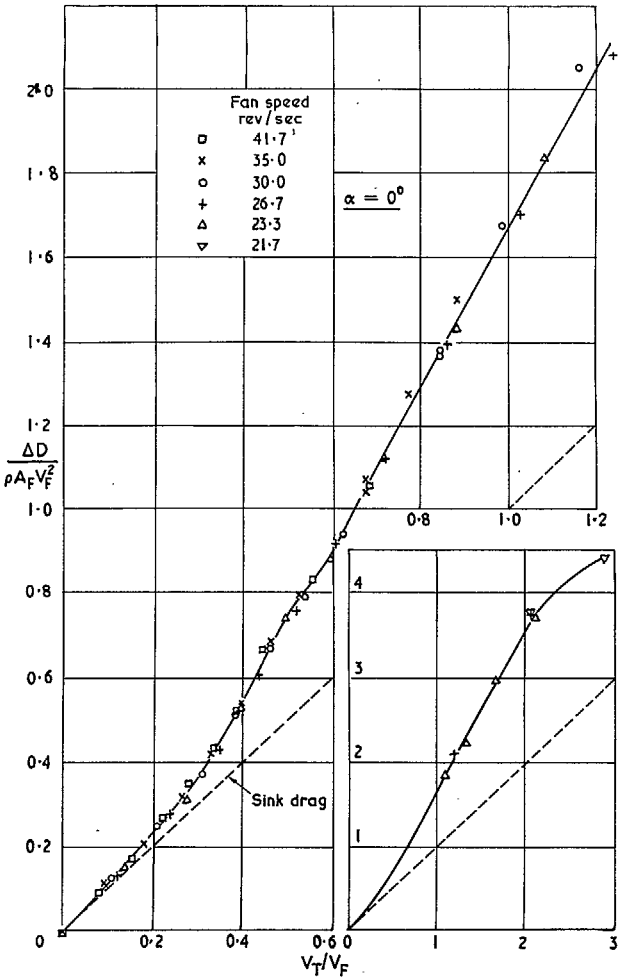

FIG. 7. Variation with forward speed ratio of the drag increment due to the fan, measured as a proportion of the momentum flux through the fan at zero wing incidence.

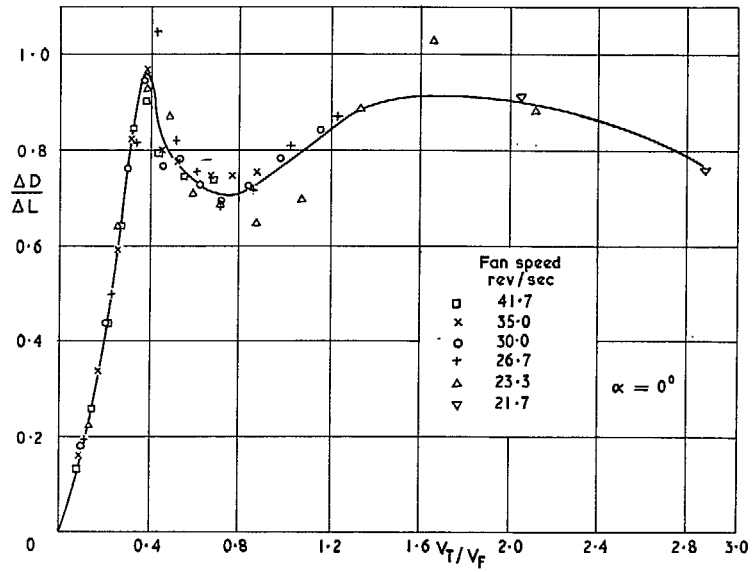

FIG. 8. Variation with forward speed ratio of the ratio of drag increment to lift increment due to fan at zero wing incidence.

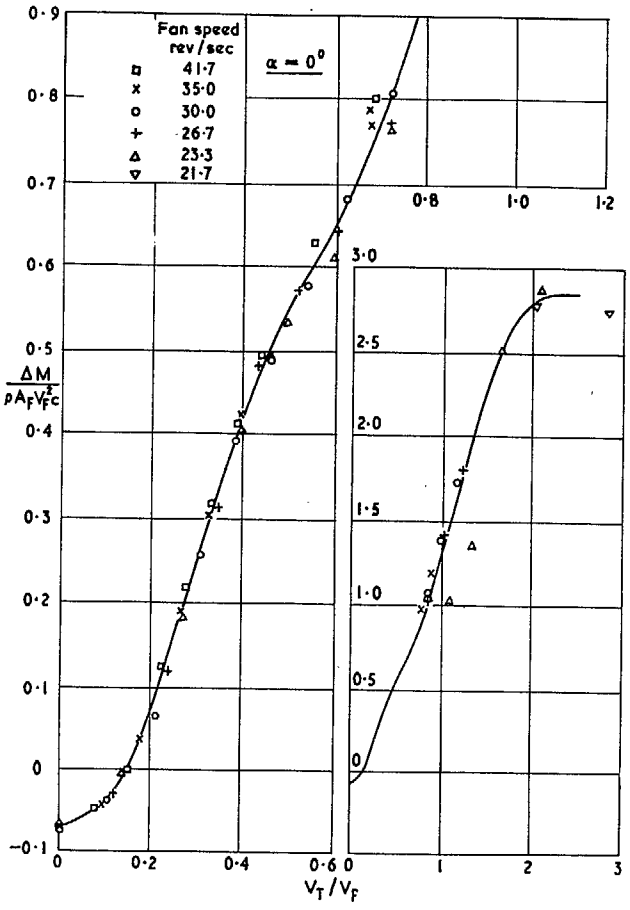

FIG. 9. Variation with forward speed ratio of the pitching moment increment due to fan at zero wing incidence.

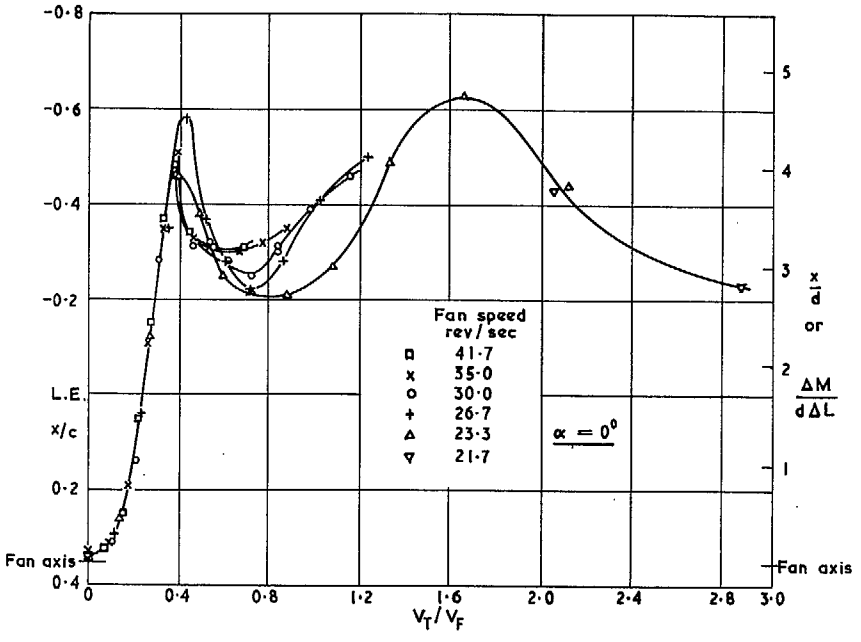

FIG. 10. Variation with forward speed ratio of centre of pressure position of the lift increment due to the fan, measured in chords relative to wing leading edge and in fan diameters ahead of fan axis, at zero wing incidence.

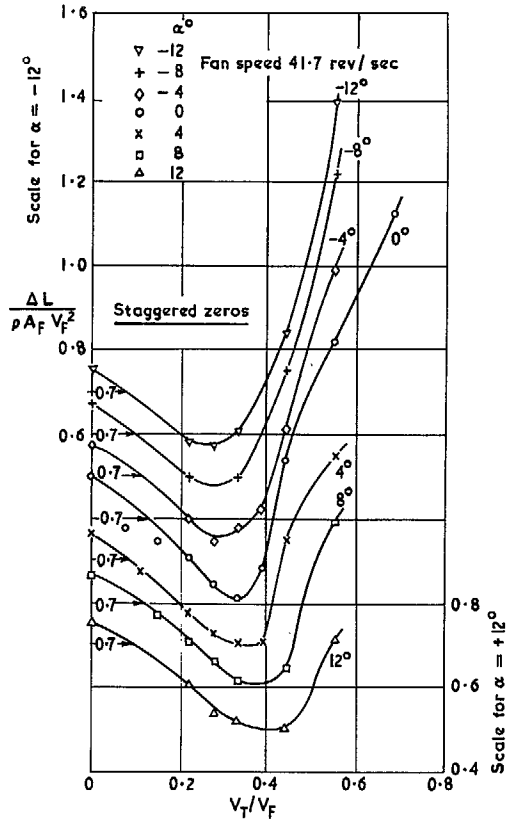

FIG. 11. Effect of incidence on relationship between lift increment due to fan and forward speed.

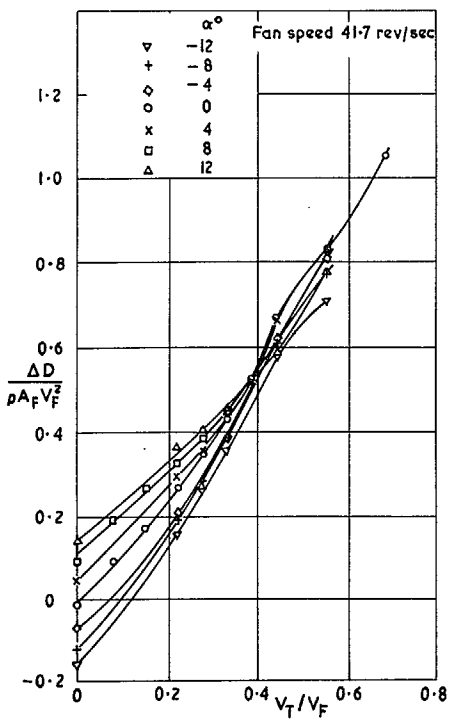

FIG. 12. Effect of incidence on relationship between drag increment due to fan and forward speed.

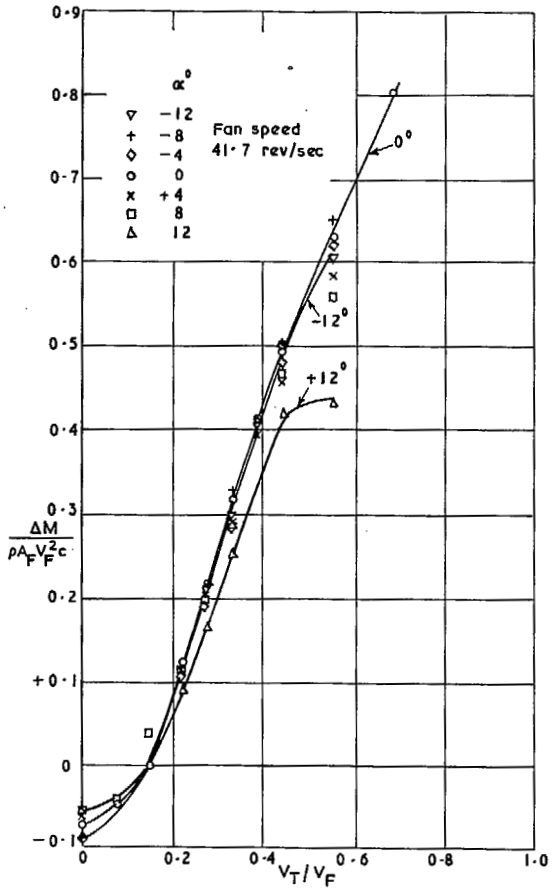

FIG. 13. Variation with forward speed ratio and incidence of the pitching moment increment due to the fan.

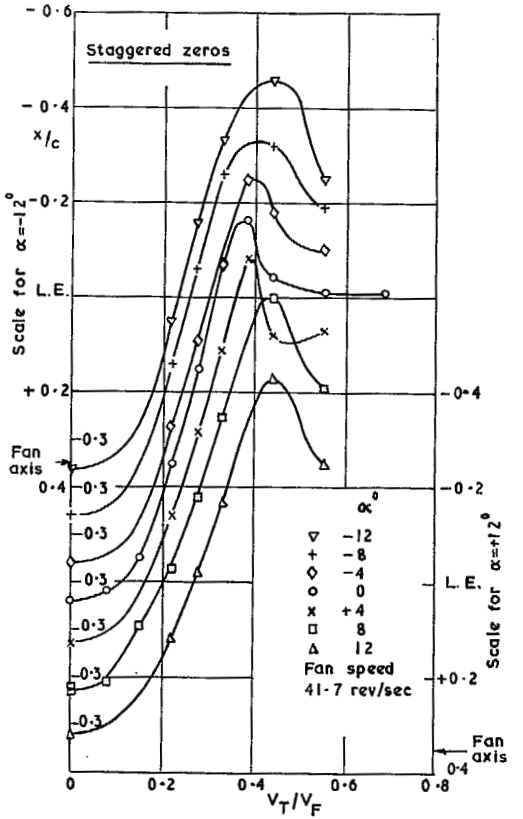

FIG. 14. Effect of incidence on relationship between centre of pressure position of the lift increment due to the fan and forward speed.

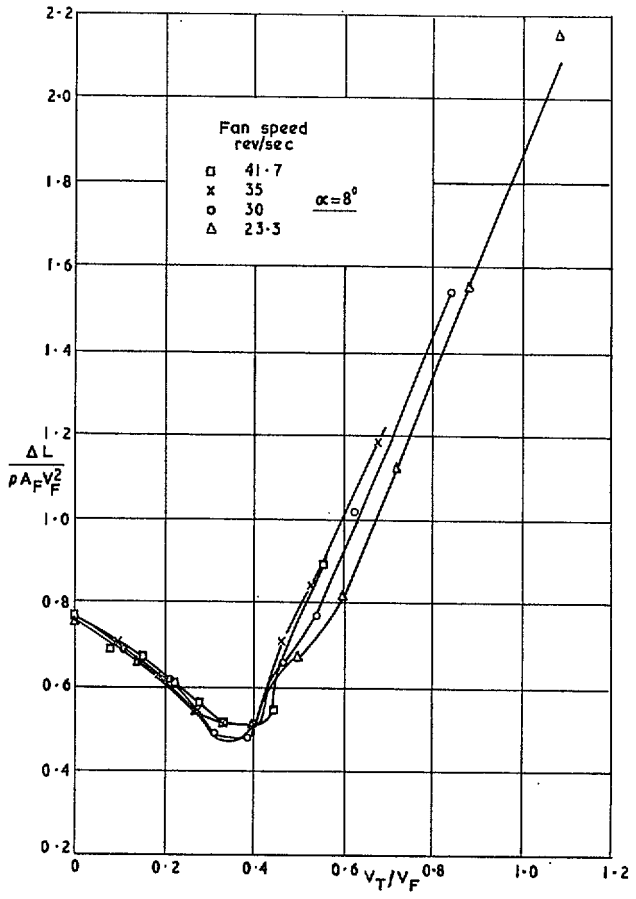

FIG. 15. Variation at 8° wing incidence of the lift increment due to the fan with forward speed ratio.

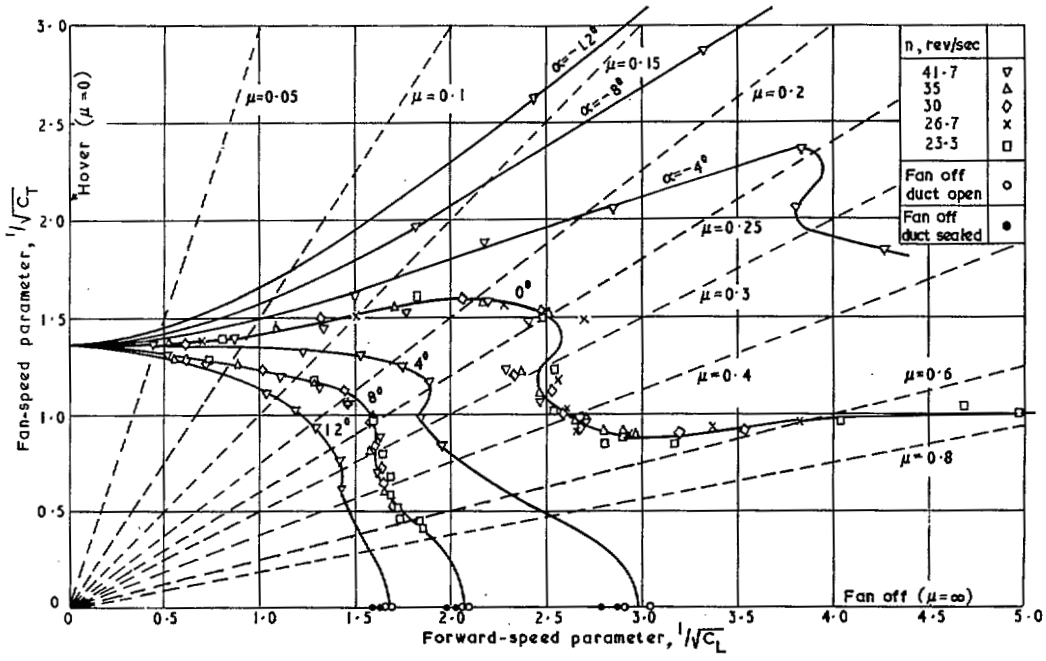

FIG. 16.
Variation of fan-speed parameter with forward-speed parameter and incidence. $A_W = 31{\cdot}1$ sq ft, $A_F = 0{\cdot}708$ sq ft, μ = Forward speed/Fan blade tip speed $= V_T/\pi nd$, $\pi nd\sqrt{(\frac{1}{2}\rho A_F/L)} = {}^1/\sqrt{C_T}$, $V_T\sqrt{(\frac{1}{2}\rho A_W/L)} = {}^1/\sqrt{C_L}$

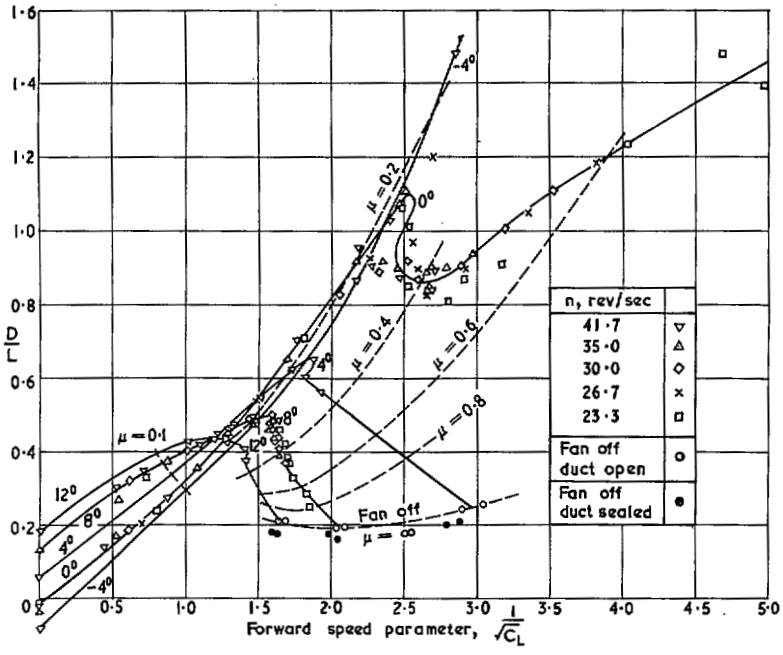

FIG. 17. Variation of drag/lift ratio with forward-speed parameter and incidence.

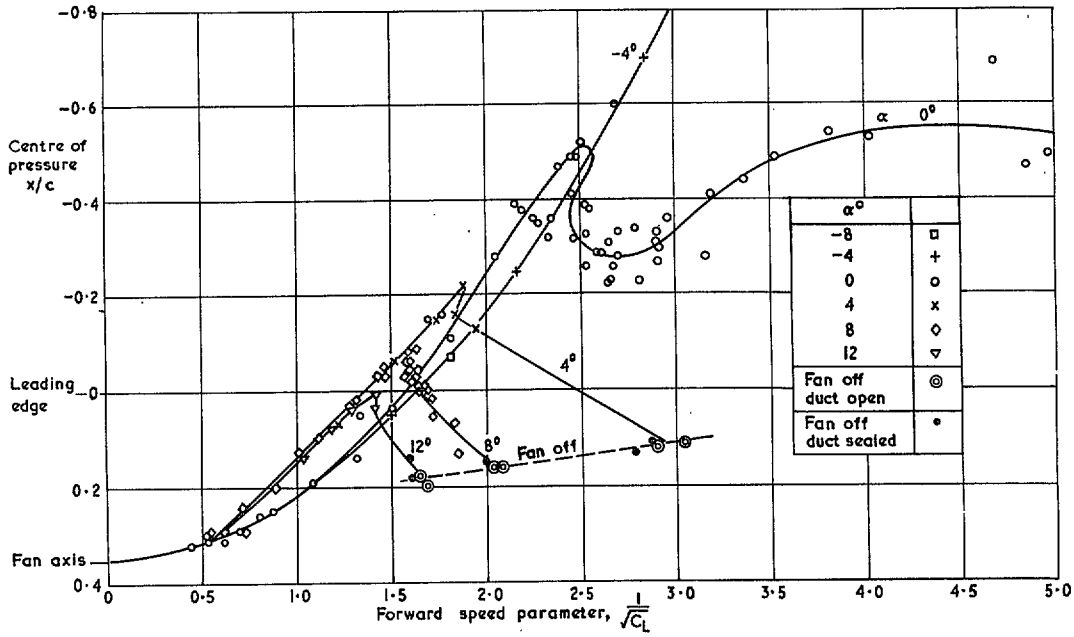

FIG. 18. Variation of centre of pressure position with forward-speed parameter and incidence.

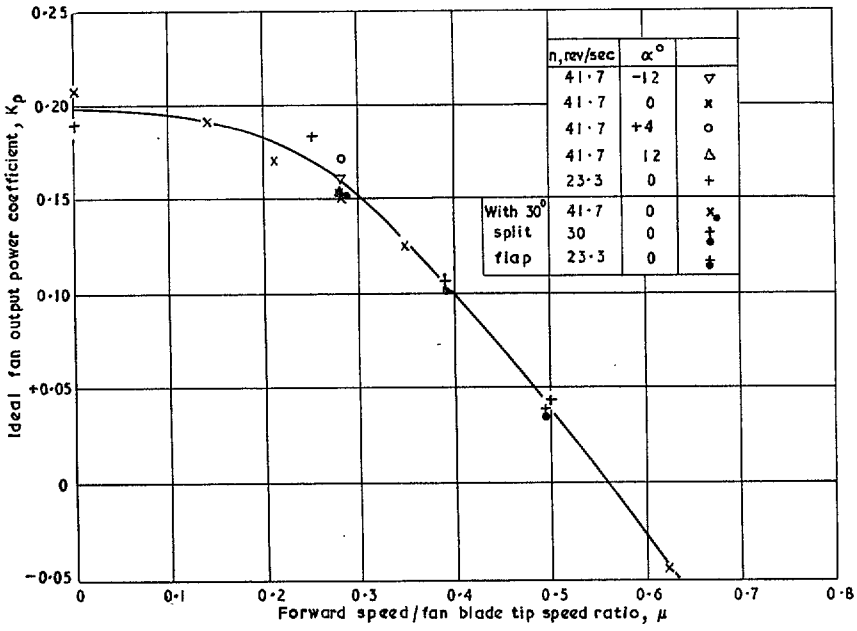

FIG. 19. Variation of ideal fan output power coefficient with forward speed/fan blade tip speed ratio. 'Ideal' signifies no entry losses.

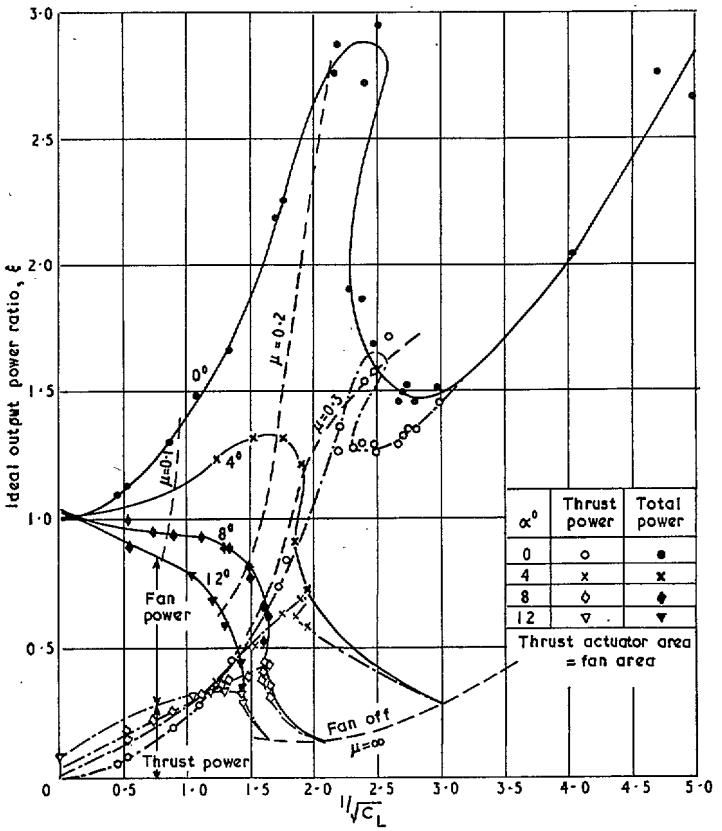

FIG. 20. Variation of ideal output power ratio with forward-speed parameter and incidence. (Thrust actuator area = fan area).

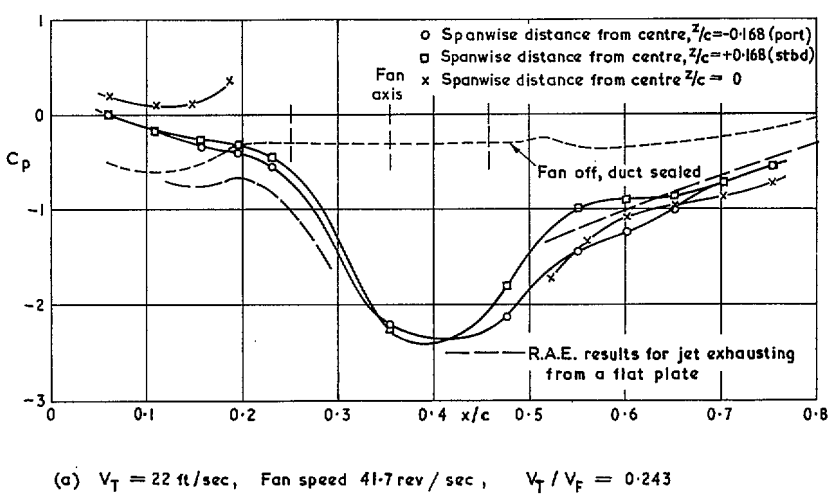

(a) V_T = 22 ft/sec, Fan speed 41·7 rev/sec, V_T / V_F = 0·243

FIG. 21a. Lower surface chordwise pressure distributions on lines through the fan axis and off centre. Zero incidence.

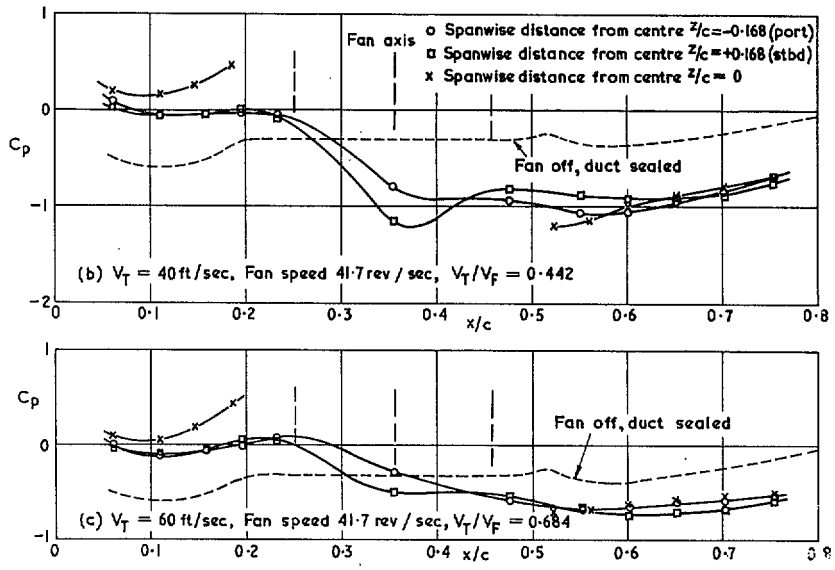

FIG. 21b & c. Lower surface chordwise pressure distributions on lines through the fan axis and off centre. Zero incidence.

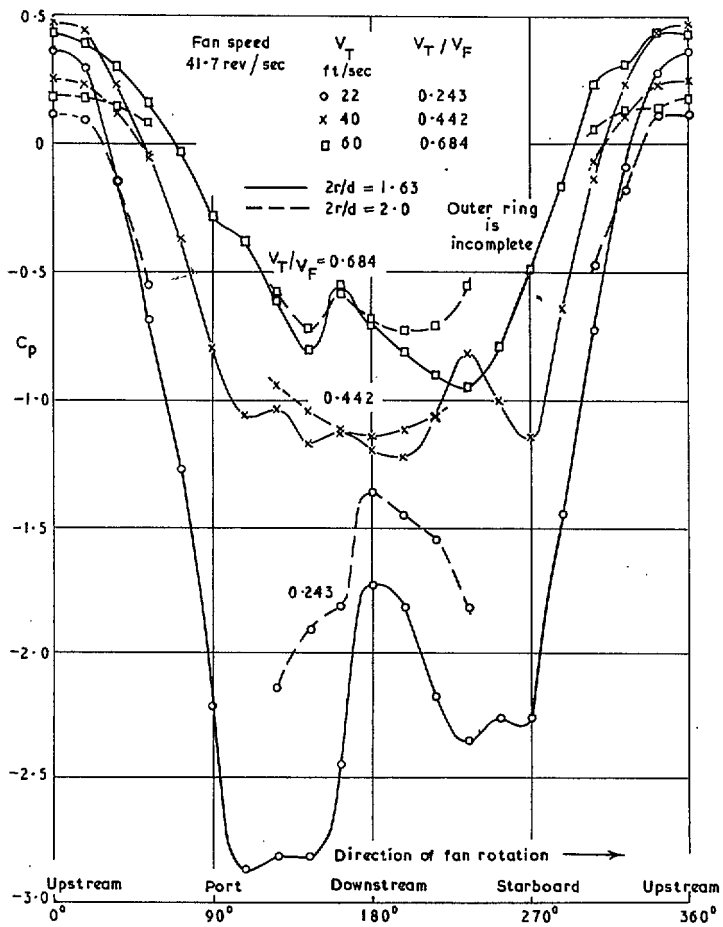

FIG. 22. Lower surface circumferential distribution of pressure at distance $2r/d$ of 1·63 and 2·0 from fan axis at three forward speed ratios.

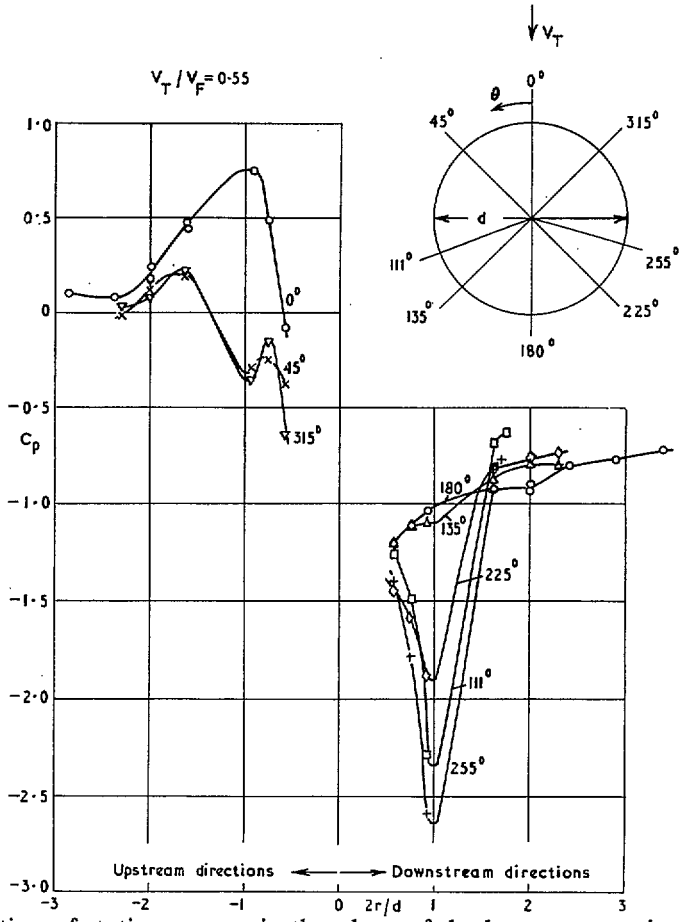

Fig. 23. Radial distribution of static pressure in the plane of the lower surface in various directions at a forward speed ratio V_T/V_F of 0·55.

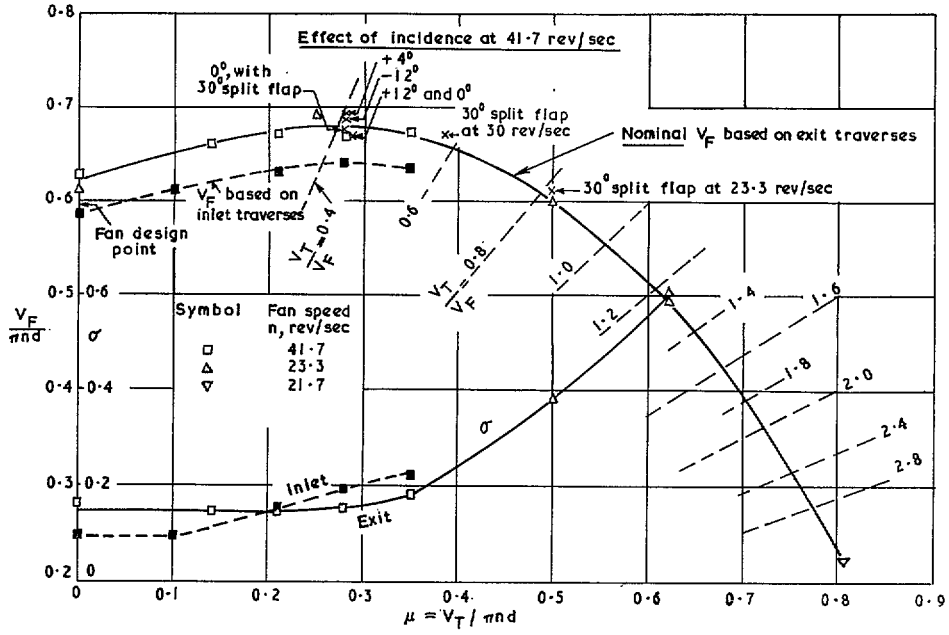

FIG. 24. Effect of forward speed (V_T) on mean flow speed (V_F) through fan and its standard deviation (σ) with plain circular entry. Zero incidence except where stated.

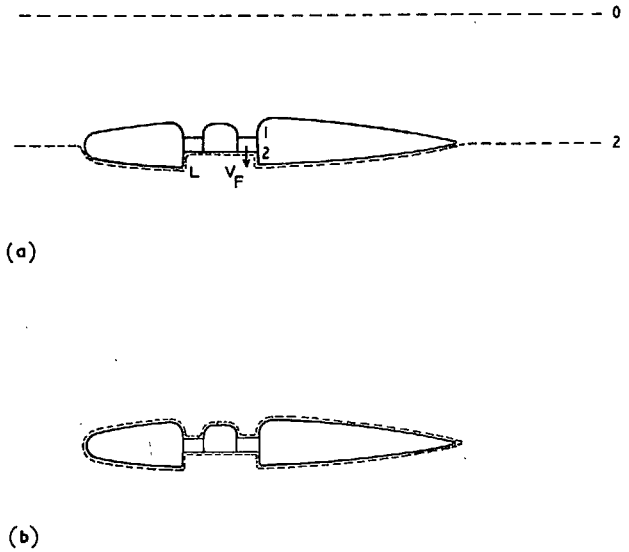

FIG. 25. Possible circuits for applying the momentum equation.

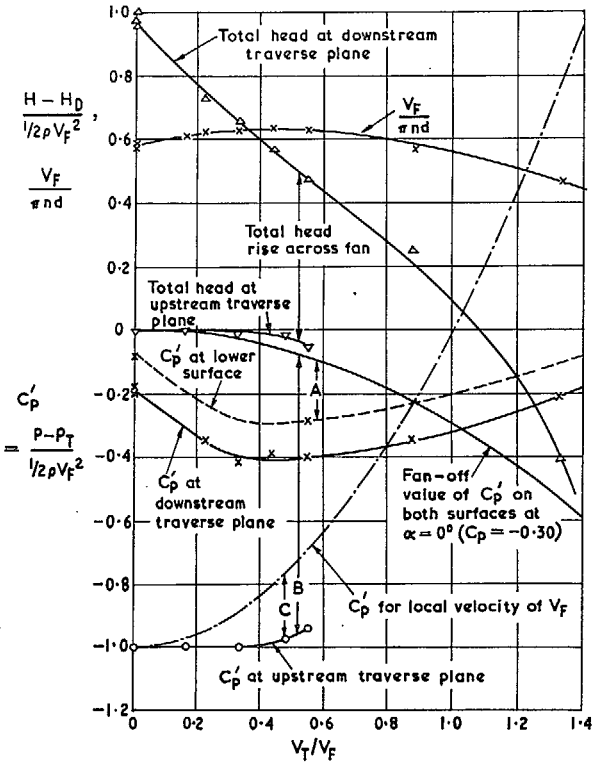

FIG. 26. Variation of mean total and static pressure levels in fan duct with forward speed ratio.

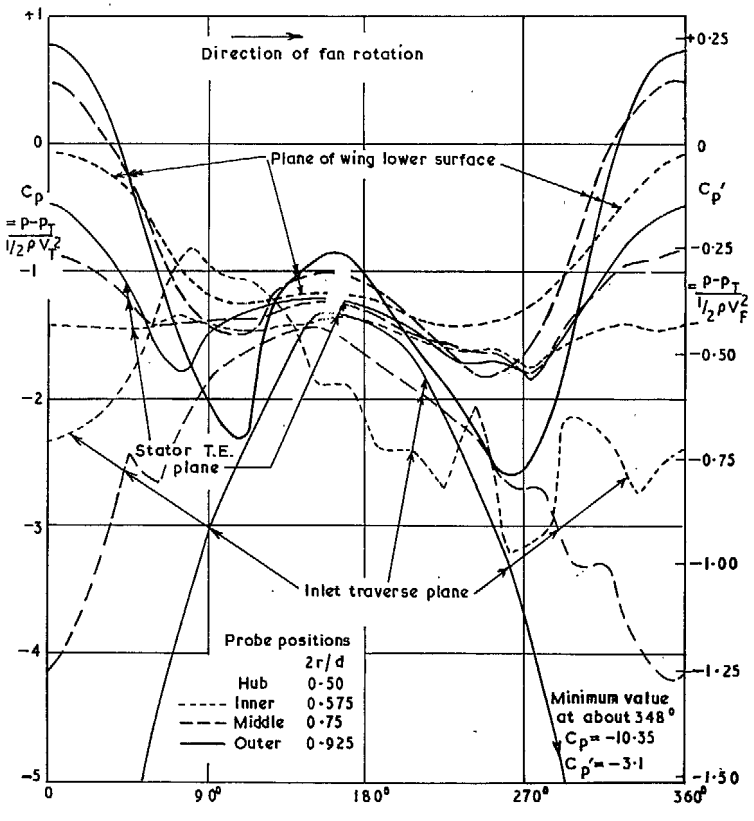

FIG. 27. Circumferential distributions of static pressure, above and below the fan and in the plane of the wing lower surface, for $V_T/V_F = 0{\cdot}55$.

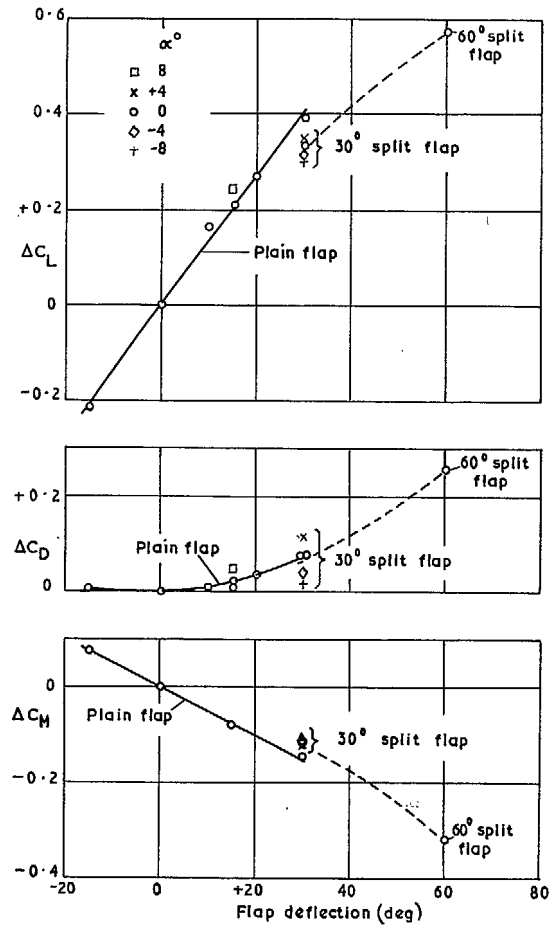

FIG. 28. Increments in C_L, C_D and C_M due to plain and split flaps with fan duct sealed.

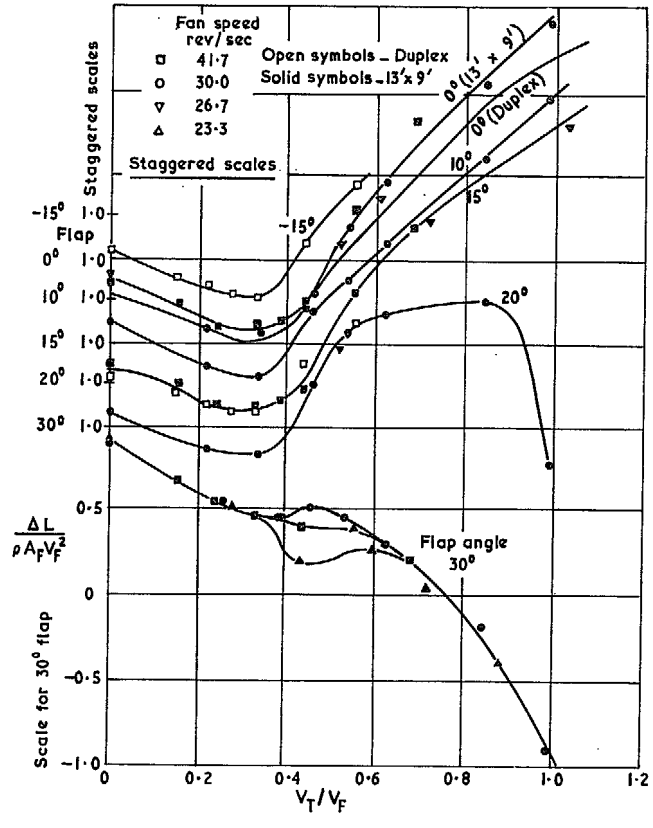

FIG. 29. Effect of plain flap deflection on the relationship between lift increment due to the fan and forward speed

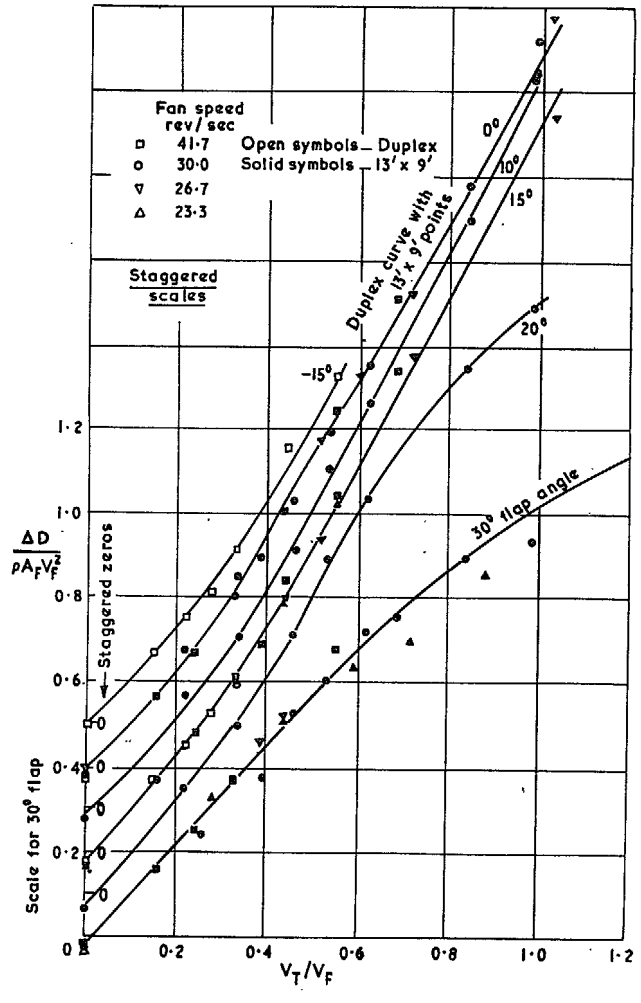

FIG. 30. Effect of plain flap deflection on the relationship between drag increment due to fan and forward speed.

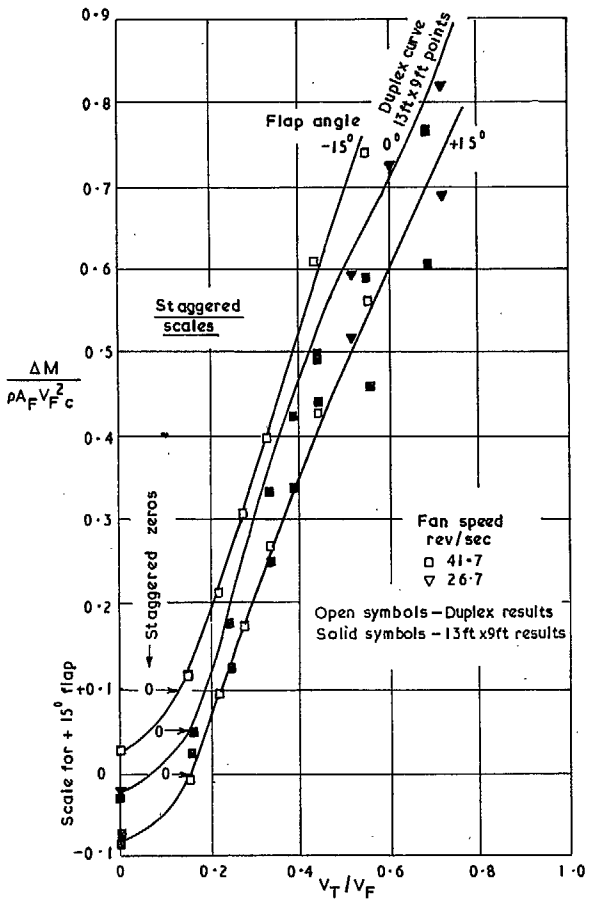

FIG. 31. Effect of plain flap deflection on the relationship between moment increment due to the fan and forward speed.

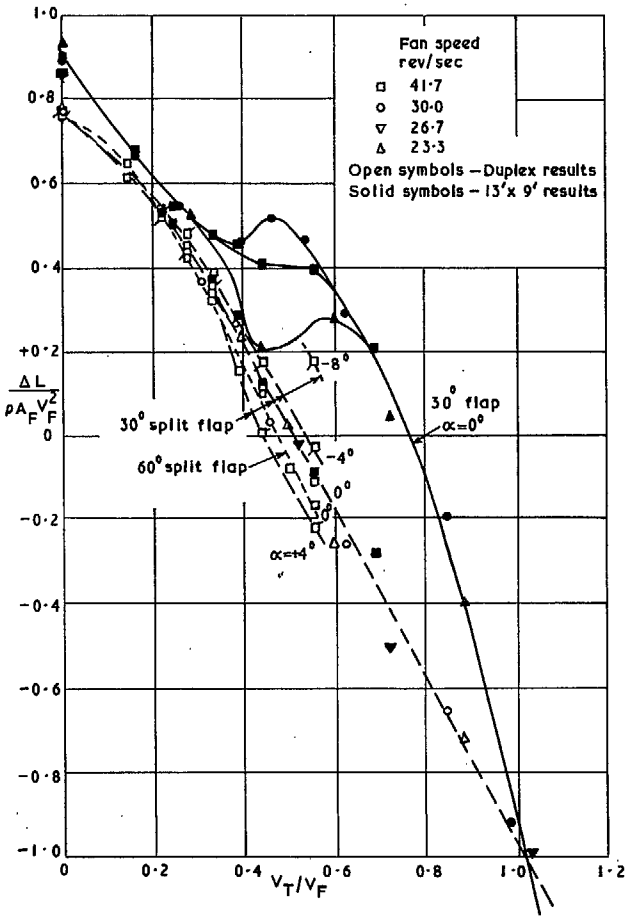

FIG. 32. Effect of split flap deflection (and variation of wing incidence) on the relationship between lift increment due to the fan and forward speed.

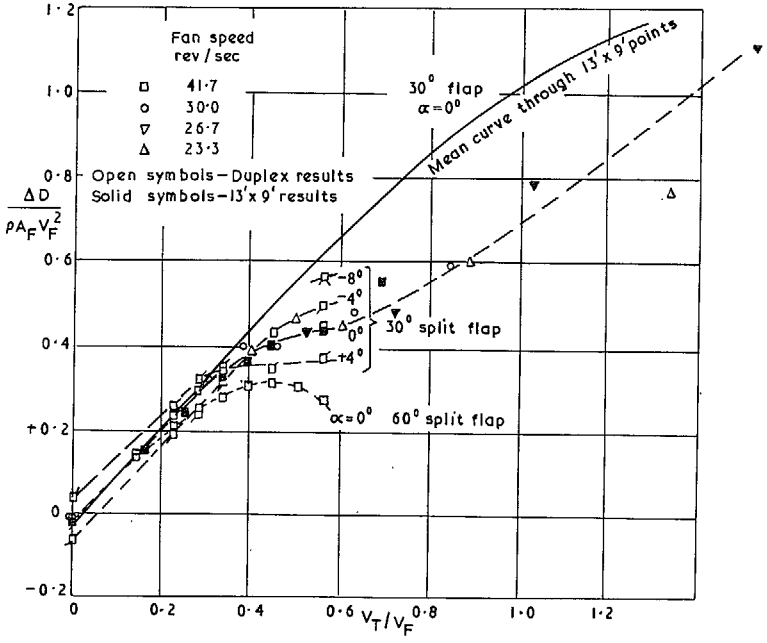

FIG. 33. Effect of split flap deflection (and variation of wing incidence) on the relationship between drag increment due to the fan and forward speed.

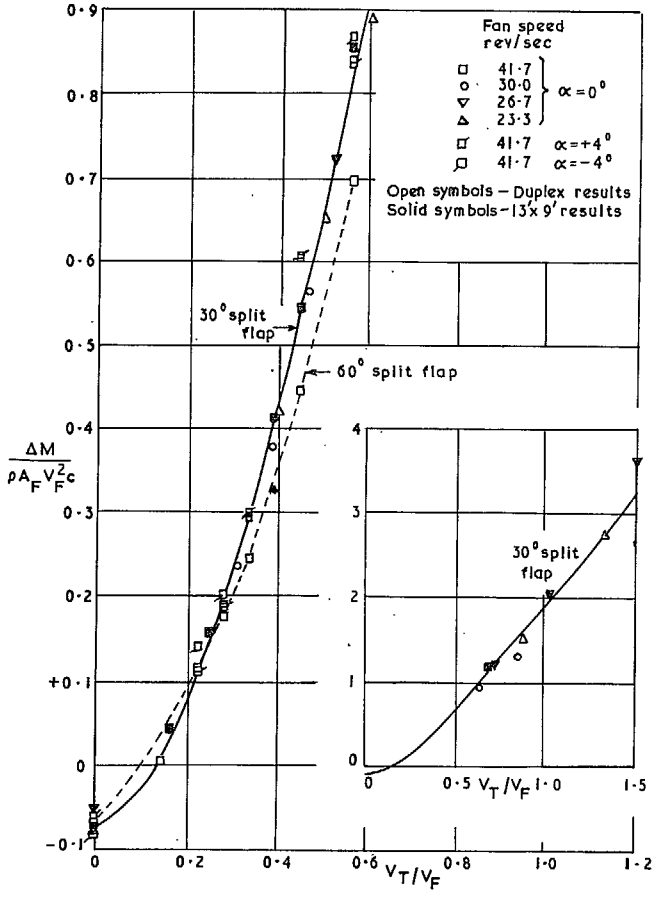

FIG. 34. Effect of split flap deflection on the relationship between moment increment due to the fan and forward speed.

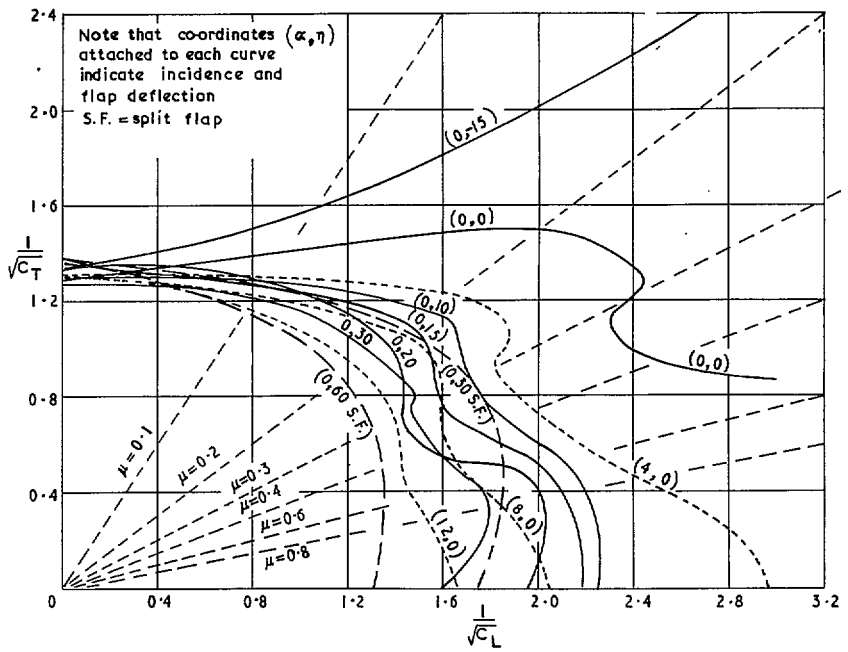

FIG. 35. Variation of fan-speed parameter with forward-speed parameter and incidence and flap deflection.

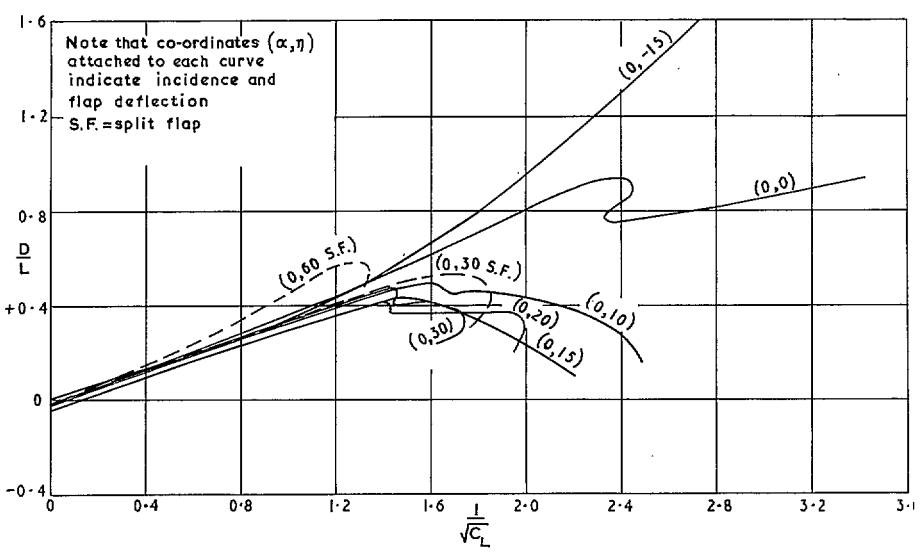

FIG. 36. Variation of drag-lift ratio with forward-speed parameter and plain and split flap deflection.

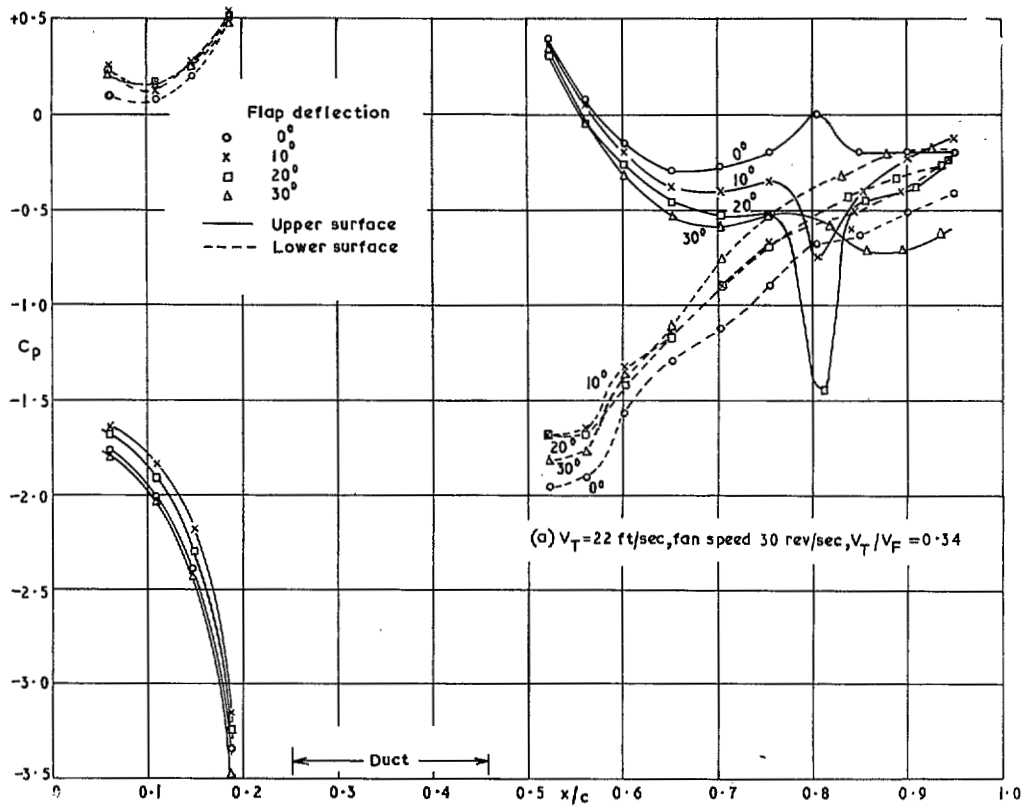

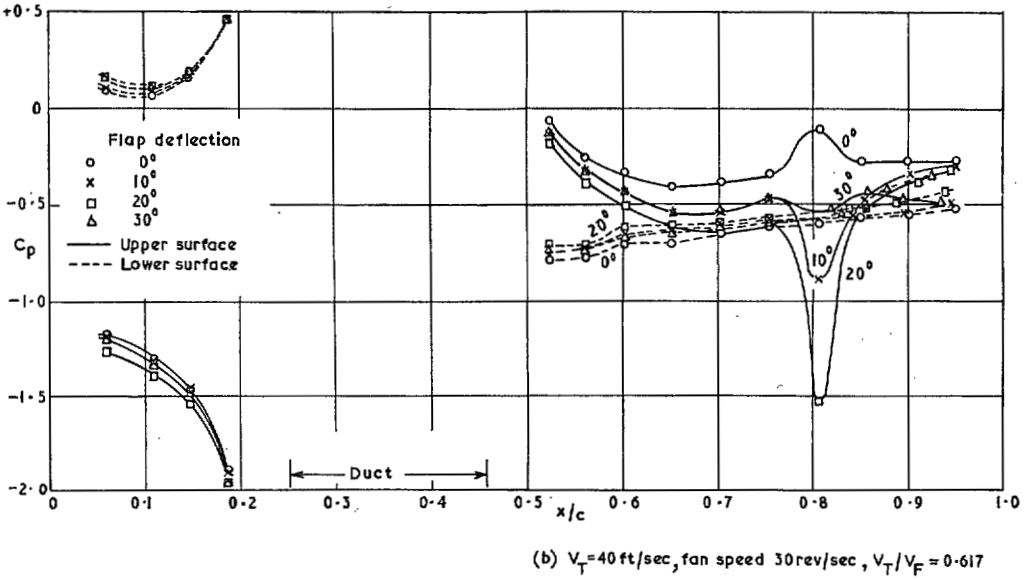

FIG. 37a & b. Chordwise pressure distribution through fan axis with plain flap.

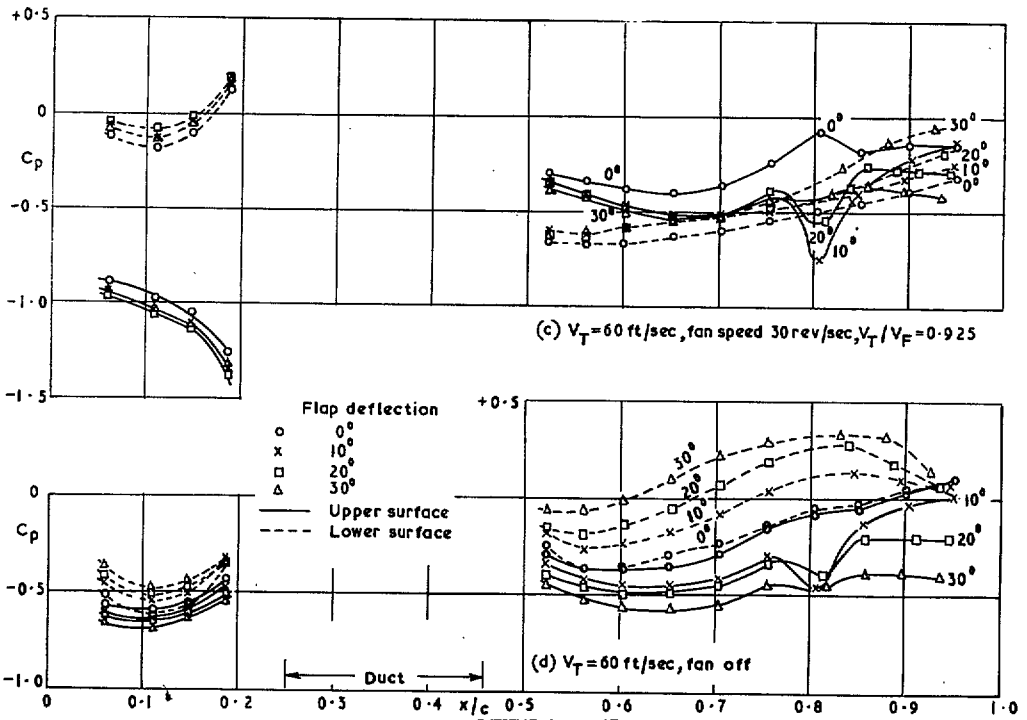

FIG. 37c & d. Chordwise pressure distribution through fan axis with plain flap.

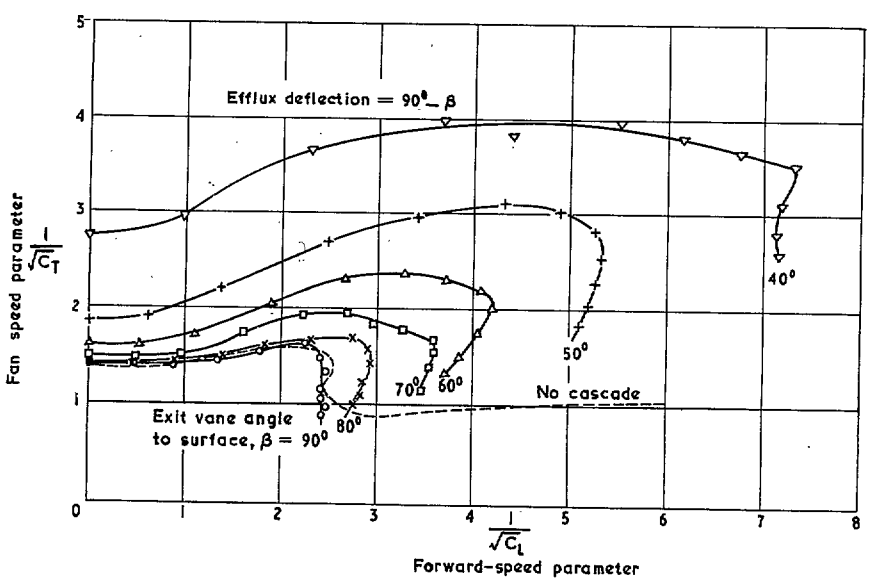

FIG. 38. Effect of exit cascade on fan-speed—forward-speed relation at zero incidence.

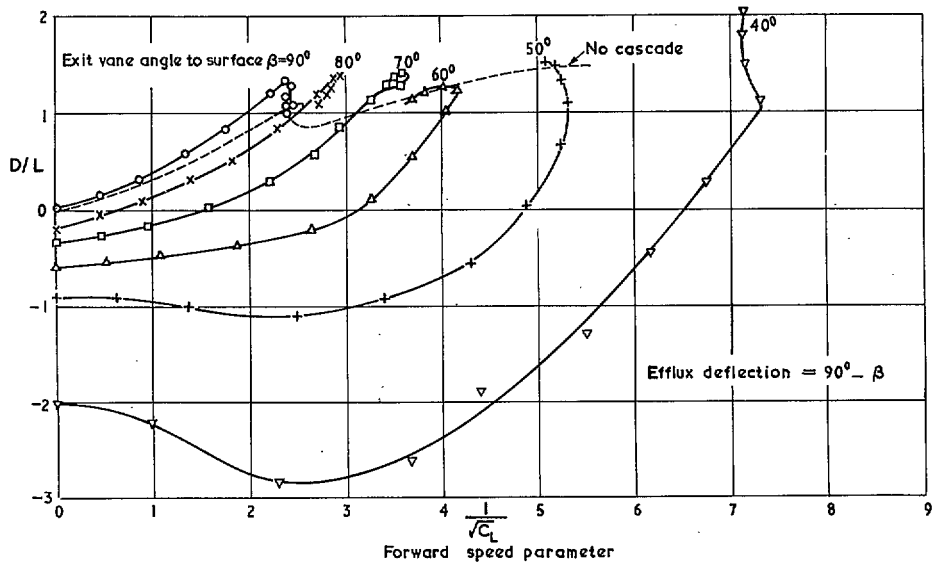

FIG. 39. Effect of exit cascade on drag at zero incidence.

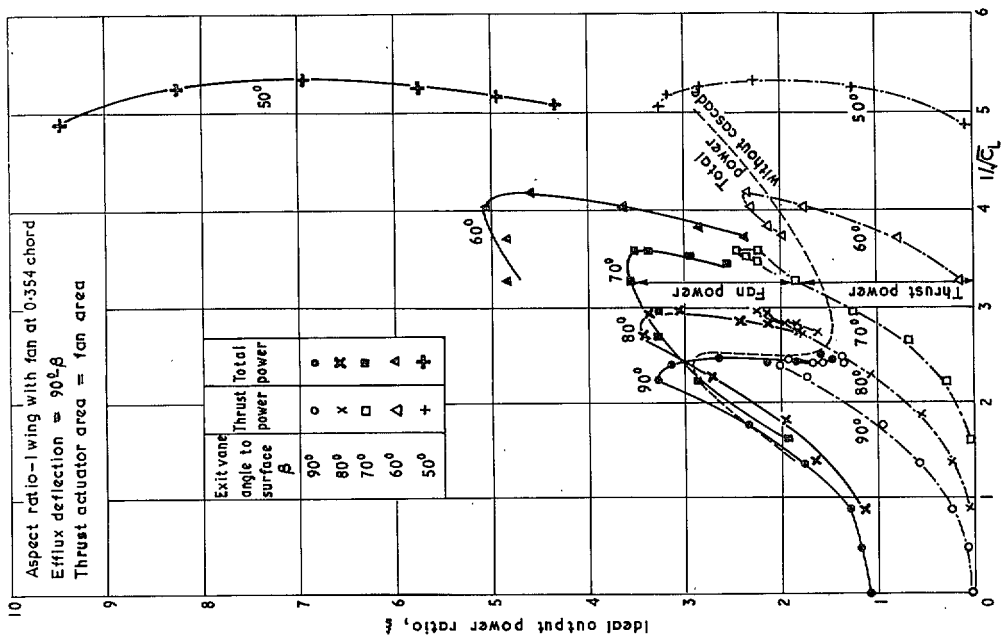

FIG. 40. Effect of exit cascade on ideal output power ratio at zero incidence.

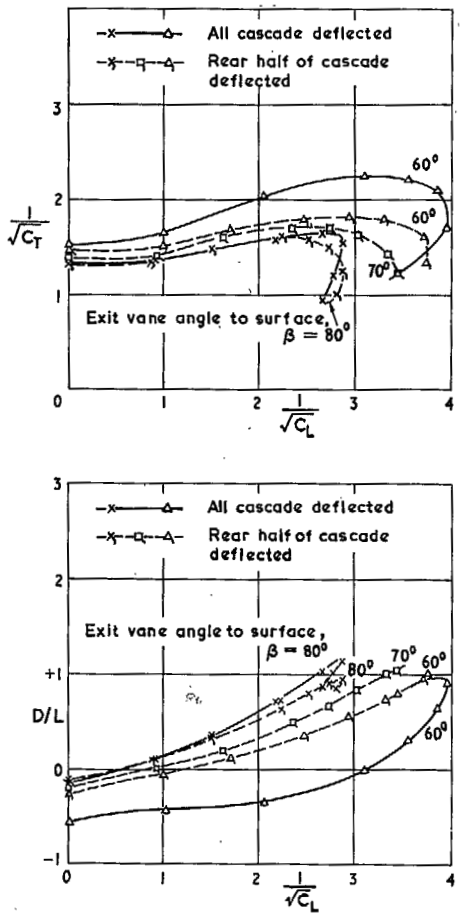

FIG. 41. Effect of deflecting rear half of exit cascade only on the variation of non-dimensional fan speed and drag/lift ratio with forward speed.

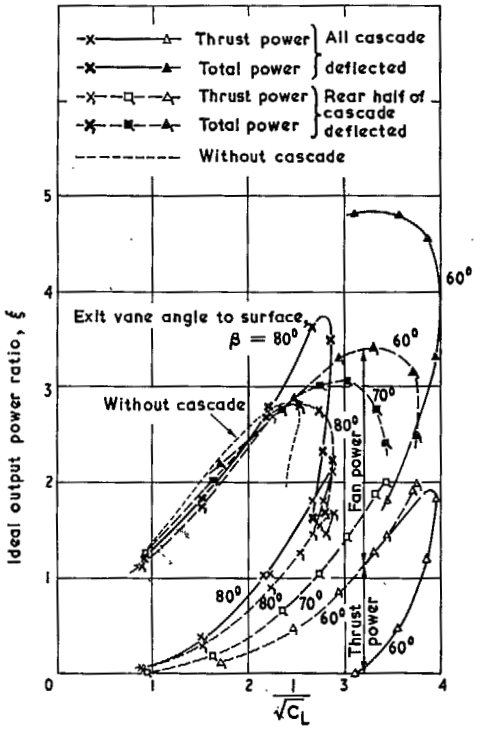

FIG. 42. Effect of deflecting rear half of cascade only on the variation of ideal output power ratio with forward speed.

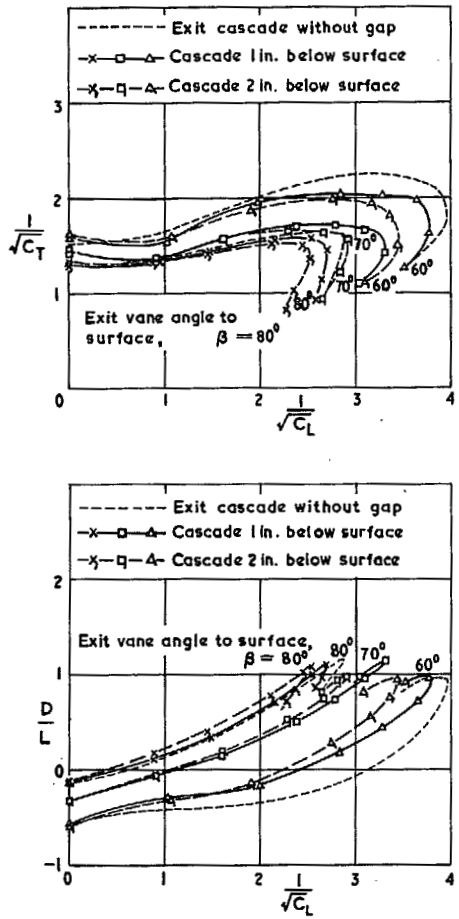

FIG. 43. Effect of lowering exit cascade 1 in. and 2 in. below surface on the variation of non-dimensional fan speed and drag/lift ratio with forward speed.

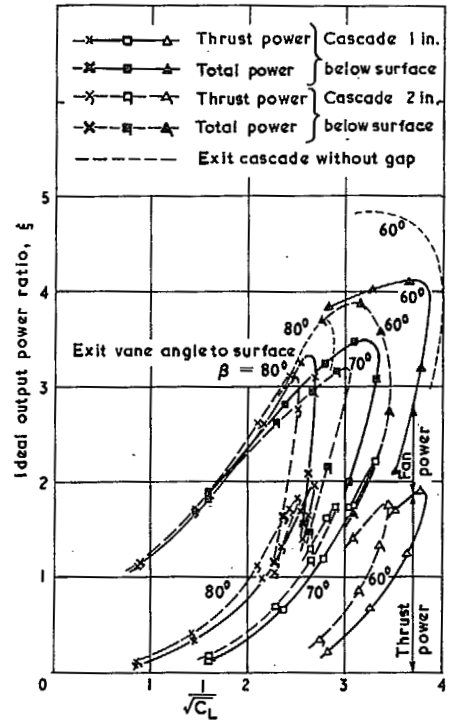

FIG. 44. Effect of lowering exit cascade 1 in. and 2 in. below surface on the variation of ideal output power ratio with forward speed.

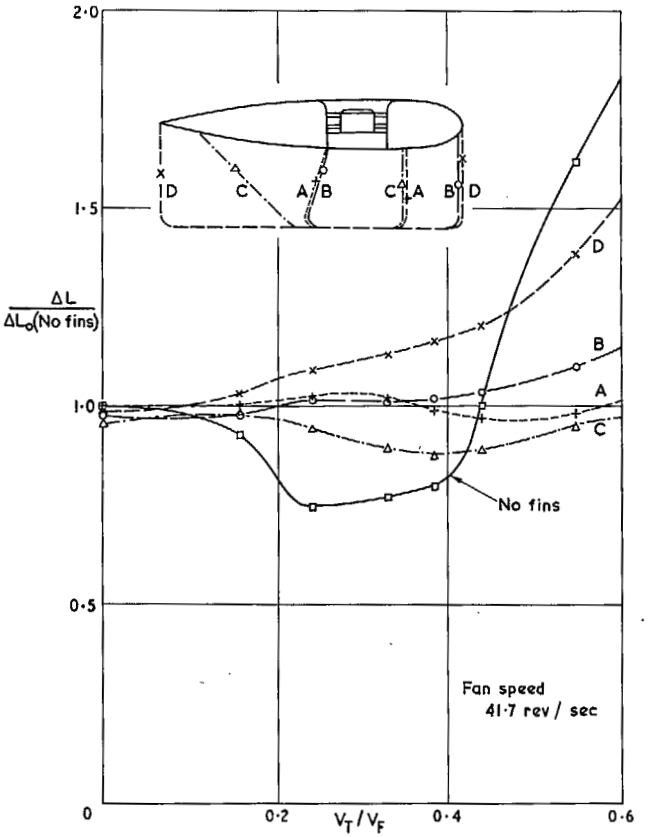

FIG. 45. Variation with forward speed ratio of the lift increment due to the fan operating in the wing with various underfin arrangements, measured as a proportion of the lift produced by the fan in static conditions without fins.

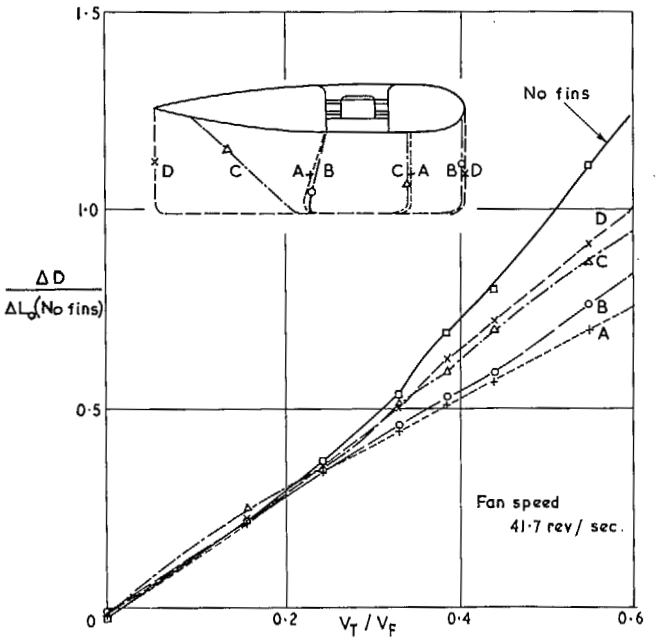

FIG. 46. Variation with forward speed ratio of the drag increment due to the fan operating in the wing with various underfin arrangements, measured as a proprtion of the lift produced by the fan in static conditions without fins.

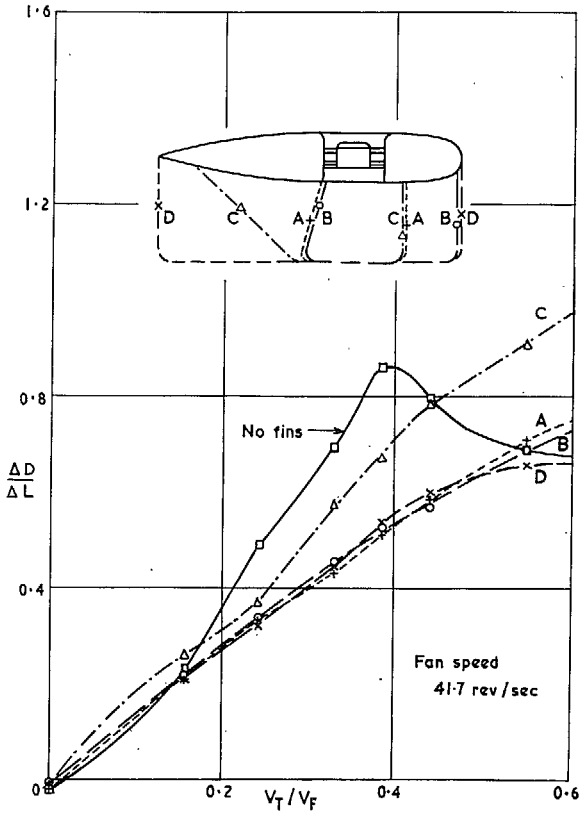

FIG. 47. Variation with forward speed ratio of the ratio of drag increment to lift increment due to the fan operating in the wing with various underfin arrangements.

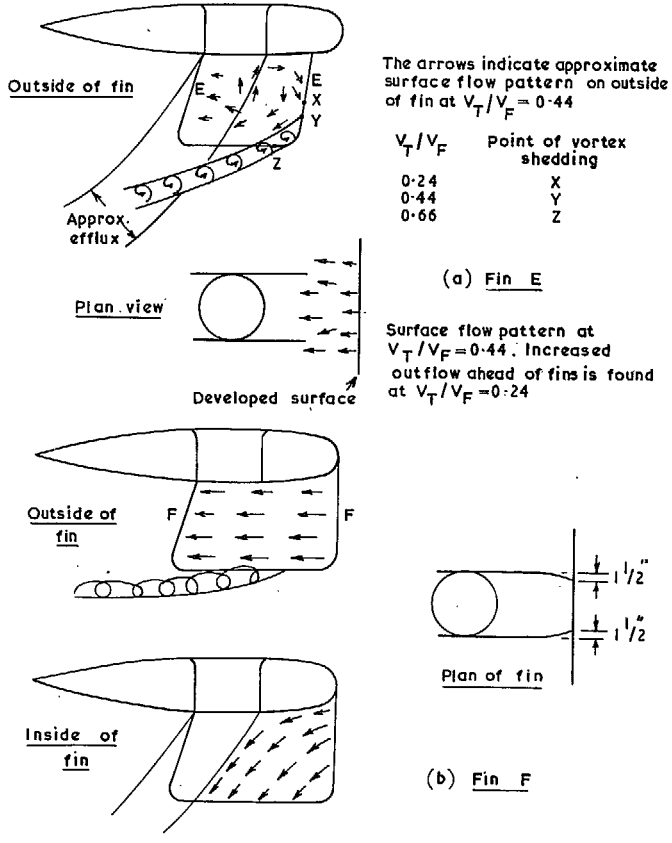

FIG. 48. Flow patterns indicated by observations of tufts on fin arrangements E and F.

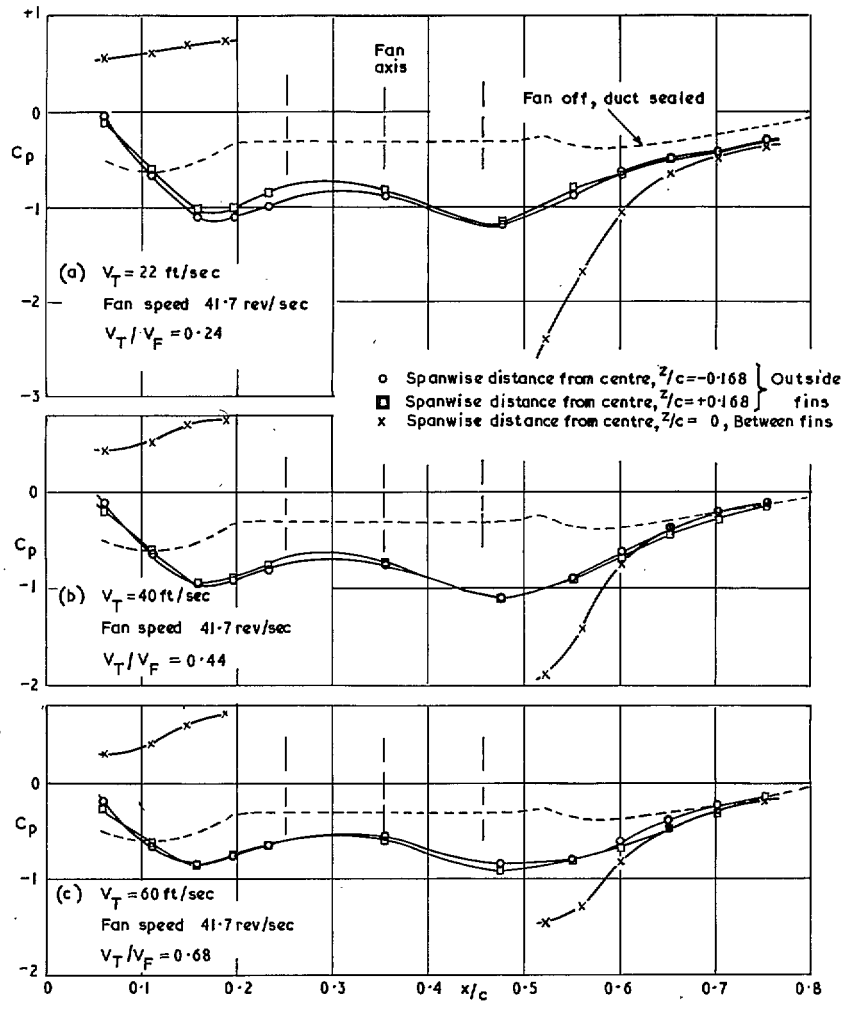

FIG. 49. Lower surface chordwise pressure distributions for wing with under-fin arrangement E. Zero incidence.

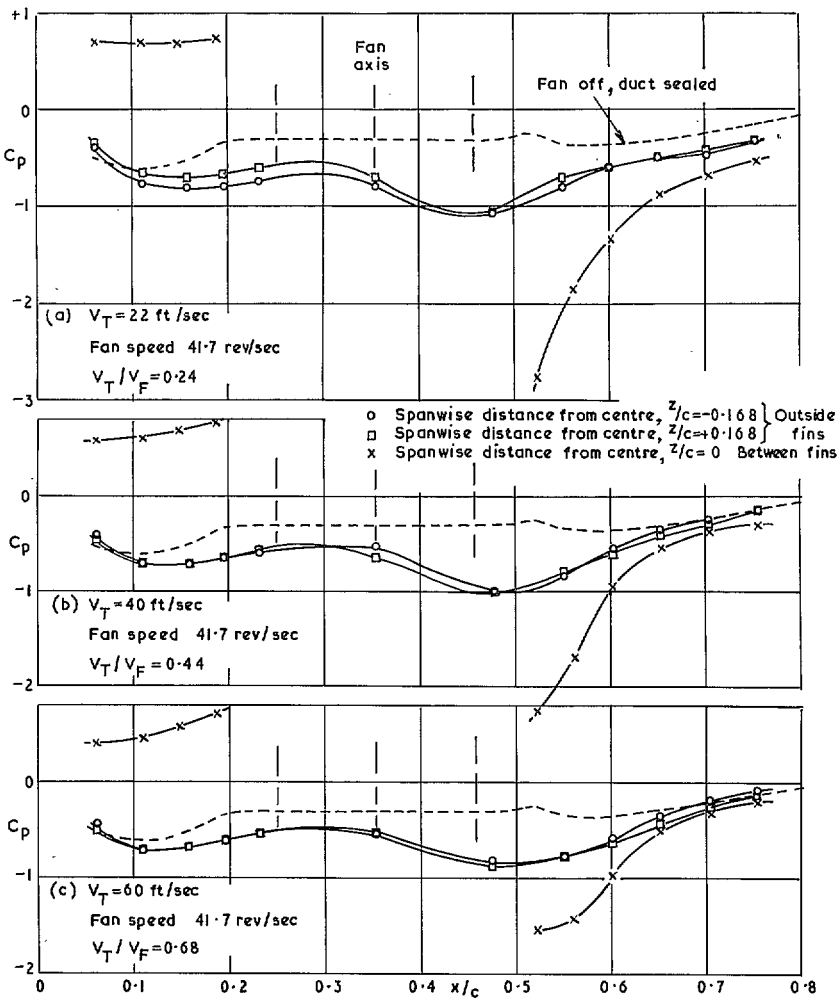

FIG. 50. Lower surface chordwise pressure distributions for wing with under-fin arrangement F. Zero incidence.

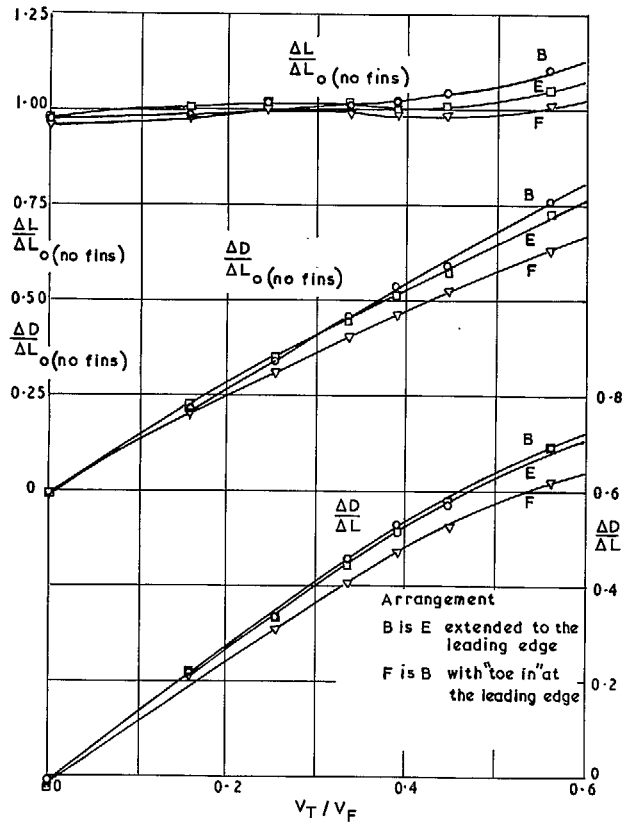

FIG. 51. Variation with forward speed ratio of the lift increment, drag increment and drag/lift ratio due to the fan operating in the wing with various underfin arrangements.

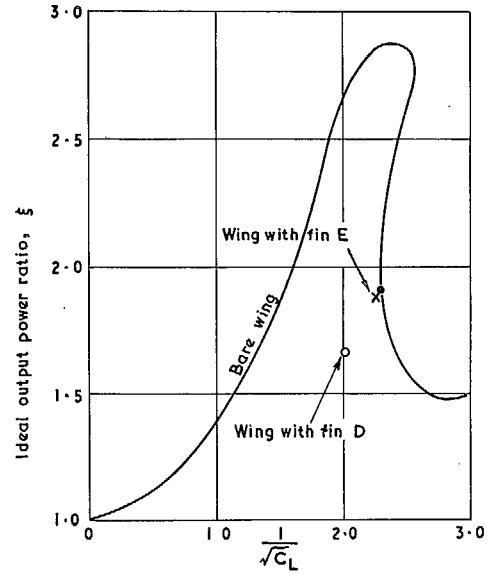

FIG. 52. Ideal power output ratios for bare wing and with fins D and E compared at $V_T = 40$ ft/sec and fan speed 41·7 rev/sec. Zero inc. Thrust actuator area = fan area.

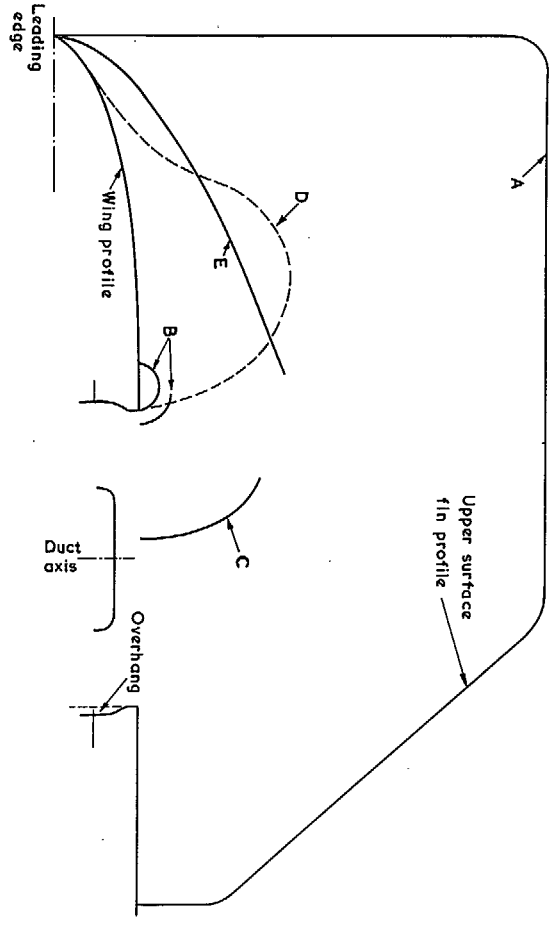

FIG. 53. Bumps and vanes tested on the inlet side of the fan duct between upper surface fins.

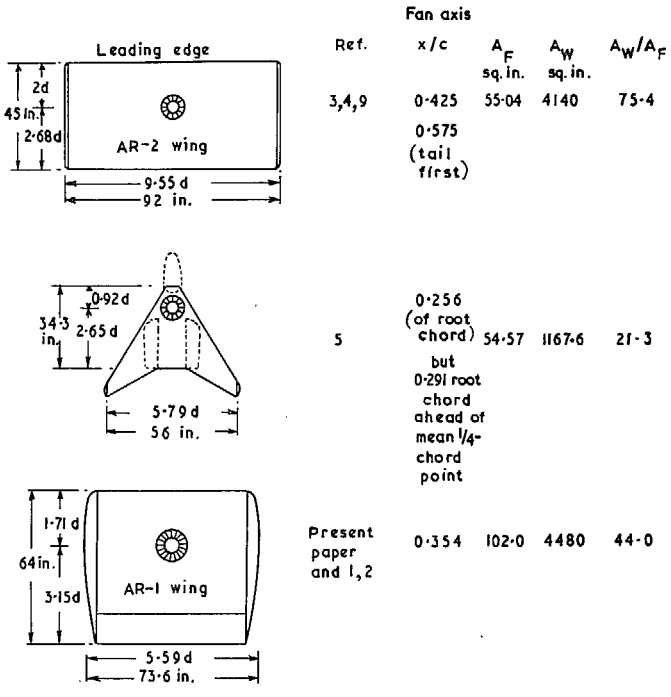

Ref.	Fan axis x/c	A_F sq. in.	A_W sq. in.	A_W/A_F
3,4,9	0·425 0·575 (tail first)	55·04	4140	75·4
5	0·256 (of root chord) but 0·291 root chord ahead of mean ¼-chord point	54·57	1167·6	21·3
Present paper and 1,2	0·354	102·0	4480	44·0

FIG. 54. Planforms and leading dimensions of the lifting fan wings tested at N.P.L.

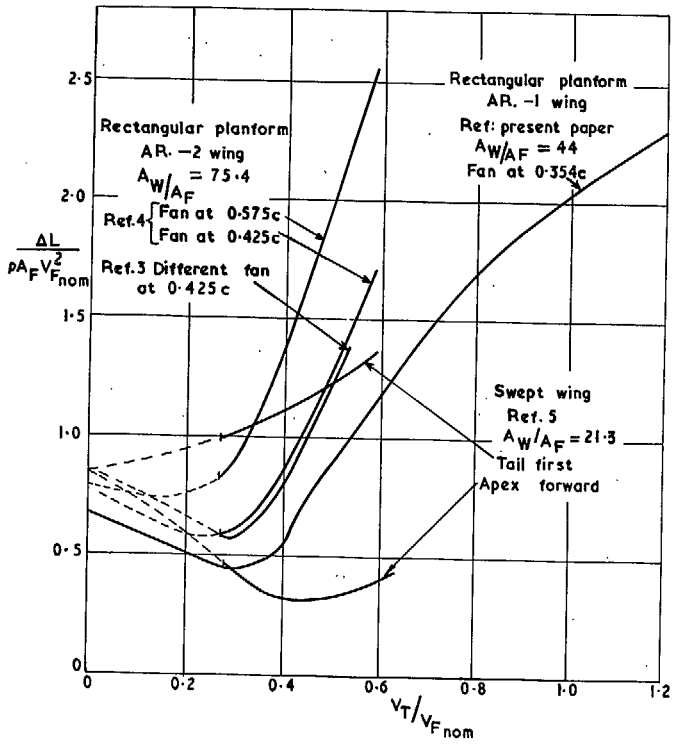

FIG. 55. Variation with forward speed ratio of the lift increment due to the fan (measured in terms of the momentum flux) for lifting fan wings tested at N.P.L.

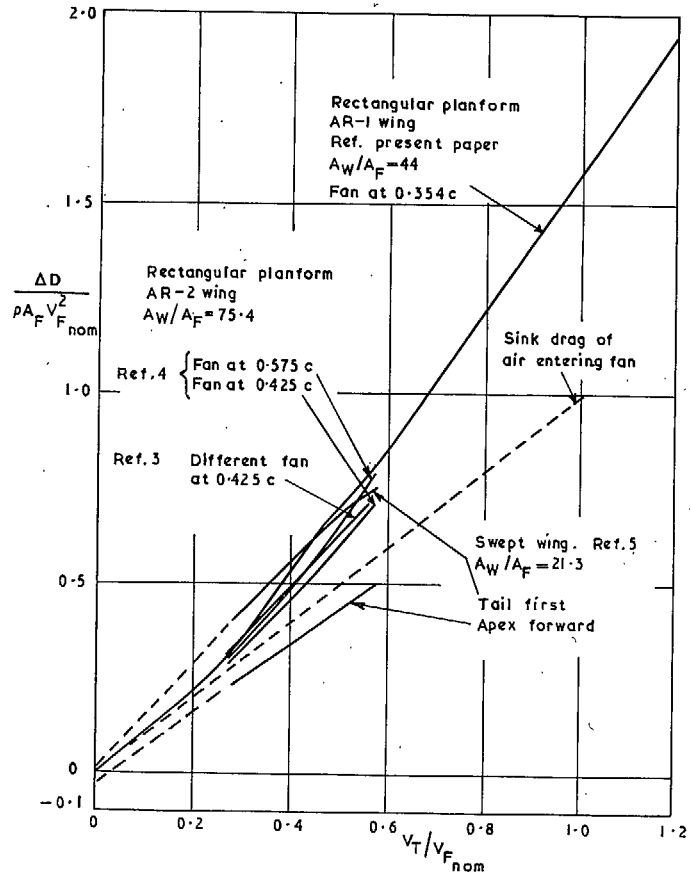

FIG. 56. Variation with forward speed ratio of the drag increment due to the fan (measured in terms of the momentum flux) for lifting fan wings tested at N.P.L.

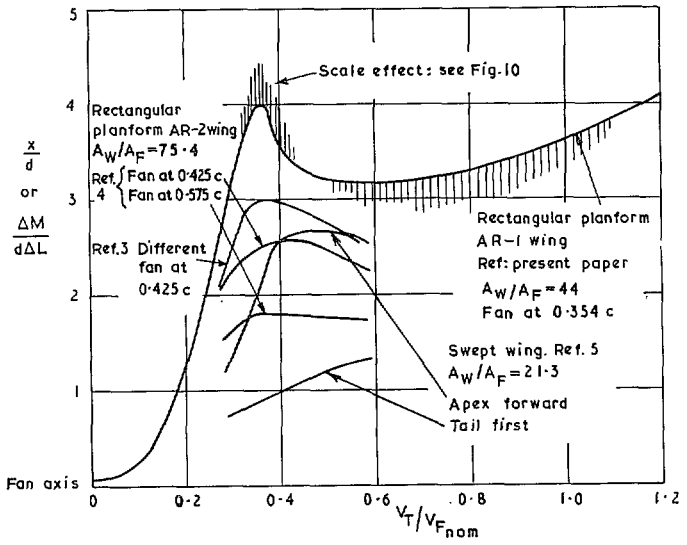

FIG. 57. Variation with forward speed ratio of the centre of pressure position of the lift increment due to fan operation (measured in diameters ahead of the fan axis) for lifting fan wings tested at N.P.L.

Printed in Wales for Her Majesty's Stationery Office by Allens (Cardiff) Limited.

Dd.125874 K5 11/66.

Published by
HER MAJESTY'S STATIONERY OFFICE

To be purchased from
49 High Holborn, London W.C.1
423 Oxford Street, London W.1
13A Castle Street, Edinburgh 2
109 St. Mary Street, Cardiff
Brazennose Street, Manchester 2
50 Fairfax Street, Bristol 1
35 Smallbrook, Ringway, Birmingham 5
80 Chichester Street, Belfast 1
or through any bookseller